AN ABSTRACT OF THE THESIS OF

William C. Kiestler for the degree of Master of Science in Nuclear Engineering presented on December 16, 1992.

Title: Design and Testing of Fabric Composite Heat Pipes for Space Nuclear Power Applications.

Abstract approved: Redacted for Privacy

Andrew C. Klein

Conventional stainless steel - water and ceramic fabric composite - water heat pipes have been built and tested. The tests have been conducted to compare the performance characteristics between conventional and fabric composite heat pipe radiators for space nuclear power heat rejection systems. The fabric composite concept combines a strong ceramic fabric with a thin metal liner to form a very lightweight heat pipe. The heat pipes tested have used identical, homogeneous fabric wicks and water as the working fluid. One fabric composite heat pipe has been constructed by fitting a braided aluminoborosilicate fabric tube over the outside of the conventional stainless steel heat pipe. A more advanced fabric composite design combines the woven fabric with a 0.25 mm (10 mil) stainless steel tube as the liner, and reduces the mass of the heat pipe by a factor of three.

A heat pipe testing facility was designed and built for the purpose of testing various conventional and fabric composite heat pipes. This facility allows the testing of heat pipes in a vacuum, at low temperatures, and can accommodate a variety of heat pipe designs. Instrumentation and computer interfacing provide for continuous monitoring and evaluation of heat pipe performance.

Tests show that heat pipe radiator capacity can be significantly enhanced by using the fabric composite design. Tests comparing a conventional heat pipe with fabric composite heat pipes achieved a 100% increase in the emissivity and heat rejection capacity of the radiator. Since the ceramic fabric is strong enough to withstand the internal pressure of the heat pipe, a very thin metal foil can be used to contain the working fluid. The increase in heat rejection capacity, combined with the significant reduction in the heat pipe mass, translates into a substantial savings for space power systems employing fabric composite heat pipe radiators.

Design and Testing of Fabric Composite Heat Pipes for Space Nuclear Power Applications

by

William C. Kiestler

A THESIS

submitted to

Oregon State University

in partial fulfillment of
the requirements for the
degree of

Master of Science

Completed December 16, 1992

Commencement June 1993

APPROVED:

Redacted for Privacy

Professor of Nuclear Engineering in charge of major

Redacted for Privacy

Head of Department of Nuclear Engineering

Redacted for Privacy

Dean of Graduate School

Date thesis is presented: December 16, 1992

Typed by William C. Kiestler

ACKNOWLEDGEMENTS

This work has been supported by the U.S. Department of Energy, Grant Number DE-FG07-89ER12901. This work represents the efforts of many individuals other than myself. I must acknowledge Tim Marks who was the co-designer of the Heat Pipe Test Facility (HPTF) and resident expert on data acquisition. Pete Meyer (Meyer's Design Shop), Steve Smith (Radiation Center), and Grant Laiblin (Willamette Hose & Fittings) contributed significantly to the design and construction of the HPTF.

I am sincerely thankful for the staff at the OSU NROTC Unit for their unwavering support. CAPT R.E. Curtis, CAPT H.M. Dyck, and in particular, LtCol Barney Grimes were incredibly gracious and supportive in letting me work on this project while teaching at the NROTC Unit. They gave me an opportunity "above and beyond," and I am very grateful.

Special thanks to L. Davis, R. Petersen, and J. Welty for their outstanding courses in heat transfer.

Dr. Andy Klein deserves the bulk of the credit for this work. I wish to thank him for being a wonderful advisor, teacher, counselor, and friend over the past two years, and for allowing me to play in the band!

Our stay in Corvallis will be especially memorable thanks to Bishop Mike Castellano, Gary Moss, and the members of the Corvallis Second Ward. 'Til we meet again.

Finally no thanks can compensate for the amount of work and effort the members of my family put in to this thesis. They have consistently supported me in all that I do, and have made it all worthwhile. Thank you, Sarah. Thank you, Shane. Thank you, Sean. Thank you, Lisa!

TABLE OF CONTENTS

LIST OF FIGURES

LIST OF TABLES

Design and Testing of Fabric Composite Heat Pipes
for Space Nuclear Power Applications

INTRODUCTION

The future exploration and use of space will rely increasingly upon the use of nuclear and other innovative power systems. The feasibility and efficiency of these systems will be measured in part by how effectively they exploit the unique space environment. Nuclear power systems have long been studied as the primary means of powering long range and remote space based missions. An integral part of any space system is a reliable and efficient means of heat transfer, for power generation, the rejection of waste heat, and temperature control. Heat pipes provide a proven mechanism for efficient heat transfer and are ideal for use in the space environment. Heat pipes have already found wide application in the space industry.

The heat pipe is a heat transfer device readily adapted to space technology. It is a device of very high thermal conductance, relatively simple design, ideally suited for radiation heat transfer, and consists of no moving parts. Advances in the design and manufacturing of heat pipes have made them even more attractive for use in space power systems. Improvements in the design and efficiency of heat pipes can significantly enhance the performance of space based power systems and may contribute significantly to their viability and cost effectiveness in the future.

The present study focuses on a specific improvement in the design of heat pipes intended to operate as efficient heat rejection devices in the unique space

environment. A "fabric composite" combines the low weight and high strength of woven ceramic fibers with a thin, lightweight metal fluid containment to create a reliable and efficient heat pipe at a tremendous savings in the system power to mass ratio. The improvement is significant since size and weight are major factors in the overall cost of space systems. Additional advantages of the fabric composite heat pipe are no less significant. The fabric composite has been shown to improve the efficiency of the heat pipe, may offer greater protection from damage due to micro meteor and space debris particles, and could be capable of compact storage and rapid post launch deployment.

A Heat Pipe Test Facility (HPTF) was designed and built to test these fabric composite heat pipes and to compare their performance with that of conventional heat pipes under conditions similar to the space environment (at low temperatures and in a vacuum). Three heat pipes were designed, built, and tested for this study. The first is a conventional water-stainless steel heat pipe using a woven aluminoborosilicate ceramic material as a concentric wick. This conventional heat pipe was tested to provide for a comparison in performance between conventional and fabric composite heat pipes. The other two heat pipes are both of the fabric composite design. A heavyweight fabric composite heat pipe was built using a stainless steel pipe with a braided aluminoborosilicate ceramic fabric tube as a sleeve over the pipe and the same material as the wick. While this heat pipe does not possess the advantages of the lightweight fabric composite design with respect to space power applications, it was tested using the HPTF to confirm the general

concept of improved emissivity. A lightweight fabric composite heat pipe was constructed using a very thin (10 mil) stainless steel tube for fluid containment and the same arrangement of aluminoborosilicate fabric as described for the heavyweight fabric composite heat pipe. This heat pipe represents a significant improvement in terms of the heat rejection power to mass ratio and was tested primarily to demonstrate the enhanced emissivity of the fabric composite condenser.

The lightweight fabric composite design concept has been proven to be feasible and has been successfully tested using the Heat Pipe Test Facility. The results of this investigation show that the fabric composite design can significantly increase the efficiency of radiant heat rejection from heat pipes. The combined advantages of improved emissivity and lower weight give the fabric composite radiator concept a promising role in space-based thermal management systems. Further development of the fabric composite heat pipe concept is suggested as a means of enhancing the viability and efficiency of future space power systems.

Chapter One discusses basic heat pipe theory and provides an historical perspective of the development of the heat pipe through literature review. Chapter Two describes the Heat Pipe Test Facility. Chapter Three consists of a detailed description of the heat pipes built and tested during this research. Chapter Four contains the results and analysis of the heat pipe tests, and Chapter Five provides conclusions and recommendations for future research. The appendices contain the essential procedures and software used during the heat pipe testing.

CHAPTER 1. LITERATURE REVIEW

1.1. Introduction

Heat pipes are devices of very high thermal conductivity. They are versatile heat transfer devices, operable over a wide range of temperatures. They can efficiently transfer heat even with a small difference in temperature between source and sink. Their simple design and reliability have made them effective heat transfer devices in a variety of engineering applications. This chapter provides a background for the development and use of the heat pipe, discusses the basic theory of operation of heat pipes, and describes the fabric composite heat pipe.

1.2. Background

Although R.S. Gaugler applied for a patent on the first heat pipe in 1942 [1], George Grover is generally given credit for the development of heat pipes for use as heat transfer devices in engineering systems. Grover, Cotter, and Erickson developed and tested heat pipe devices in 1963 and first suggested the term "heat pipe." Grover described the heat pipe as a "synergistic engineering structure," exhibiting a thermal conductivity much greater than known metals. He also recognized their potential for use in space [2]. With the publication of his paper "Structures of Very High Thermal Conductance," Grover introduced a field of heat transfer technology that has expanded dramatically and produced a number of

significant practical applications. Today, the theory of heat pipes and their application in engineering systems is well studied and documented.

Heat pipe technology developed first, and most rapidly, within the space industry. Engineers were quick to acknowledge the potential for the use of heat pipes for waste heat rejection in space power systems, and for the continuing problem of spacecraft temperature control. In a communication to the *Journal of Applied Physics* in 1963 Grover stated, "We have no reason to doubt that heat pipes will work under gravity-free conditions and, therefore, should have important applications in space." Grover's initial interest was in the use of sodium liquid metal heat pipes for heat transfer in space based thermionic reactors [3]. He had exceptional vision, as the use of heat pipes for heating of thermionic emitters and cooling of thermionic collectors continues to be a primary consideration for their use in space power systems.

Important work in the development of liquid metal heat pipes was conducted at Los Alamos in the 1960's [4]. This research produced a wealth of empirical data on the feasibility, materials compatibility, operational limits, and behavior of high temperature liquid metal heat pipes. The dynamics and theory of operation of heat pipes was outlined by Cotter in 1965 [5], and the work of Deverall, Kemme, and others at Los Alamos, led to the first successful zero gravity test of a heat pipe in 1967 [6]. After the success of the zero gravity test, heat pipes were used in a variety of space applications, including the temperature control of satellites and the cooling of radioisotope thermal generators (RTG) used to power deep space probes

[7]. An excellent summary of the work conducted at Los Alamos is contained in Reid [4].

Among the most significant of the early space applications was the SPAR reactor, a space based thermoelectric power system. The SPAR program, the forerunner to the current SP-100 space power program, proposed the use of heat pipes for performing several functions within a thermionic reactor power system. The SPAR, shown in Figure 1.1, uses three sets of heat pipes. Sodium - molybdenum heat pipes transfer heat from the reactor core to a set of potassium - niobium heat pipes, which are coupled to the radiator. The radiator consists of an array of potassium - titanium heat pipes that radiate the reactor's waste heat to space [8].

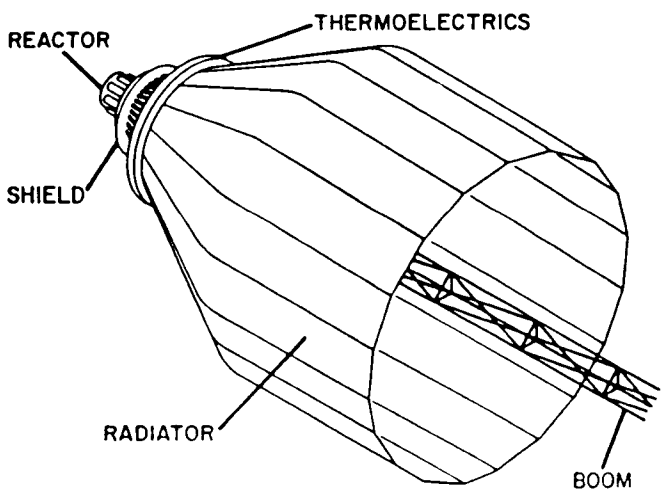

Figure 1.1. The SPAR Space Power System [8].

As part of a renewed effort to develop a feasible space reactor power system for use in future space applications, design of the SP-100 space power system began in 1983 [9]. The SP-100 is a versatile power system capable of providing power from 10 kWe to 100 kWe. This flexibility has made the SP-100 a candidate for use in a variety of future space applications, including space stations and lunar bases. In the SP-100, thermal energy is produced in a fast spectrum reactor and converted to electrical energy by a thermoelectric energy conversion unit. The reactor is cooled by magnetically pumped liquid lithium, and waste heat is rejected by an array of titanium-potassium heat pipes. The general configuration of the SP-100 is shown in Figure 1.2. The heat rejection subsystem is shown in Figure 1.3.

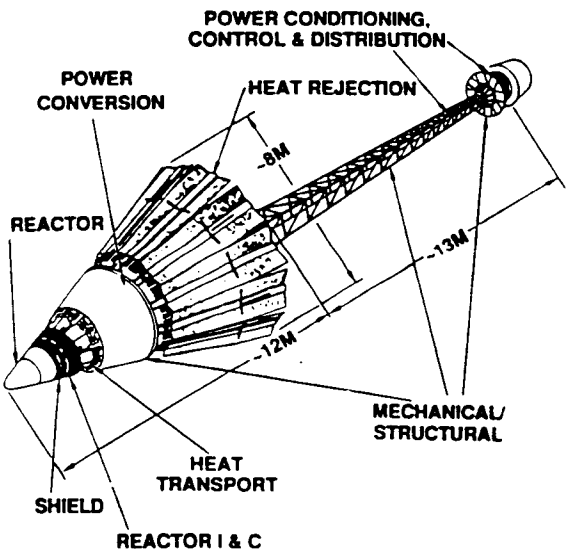

Figure 1.2. The SP100 Space Power System [9].

The titanium-potassium heat pipes provide for a reliable and efficient means of waste heat rejection and operate in a temperature range of 750 to 850 K. The SP-100 heat pipe radiator uses a carbon-carbon composite to provide protection for the heat pipes against micrometeoroids [9].

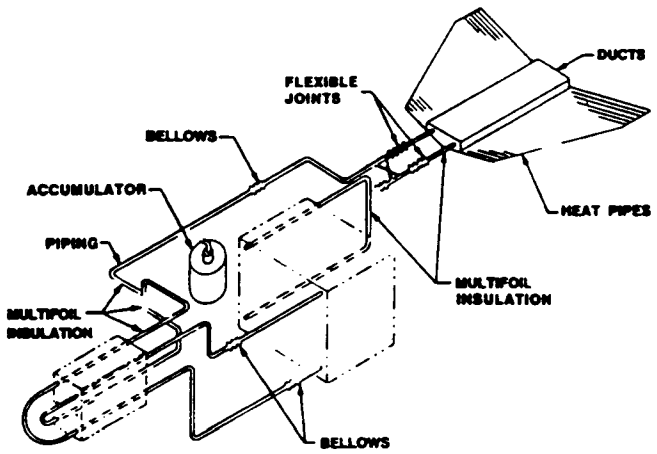

Figure 1.3. The SP100 Heat Rejection Subsystem [9].

More recently conceived designs of space power systems also use heat pipes. Examples of these designs are the Small Externally-fueled Heat Pipe Thermionic Reactor (SEHPTR) [10] and the Moderated Heat Pipe Thermionic Reactor (MOHTR) [11]. The SEHPTR, shown in Figure 1.4, is a thermionic power system capable of providing both electric power and propulsion. A uranium oxide fuel, clad with tungsten, provides heat to a converter device called the Thermionic Heat Pipe Module (THPM). The THPM (Figure 1.5) consists of two

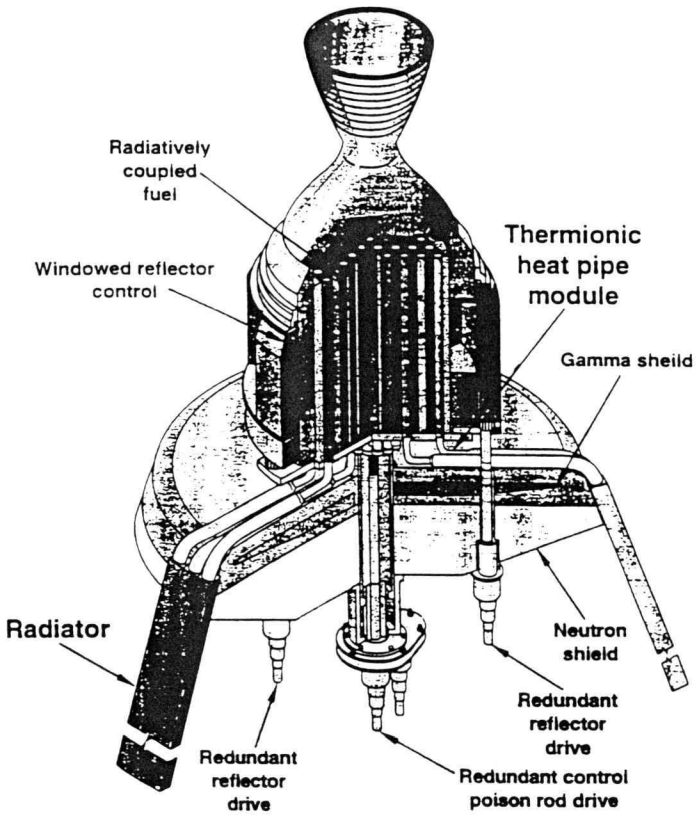

Figure 1.4. The SEHPTR Stage [12].

concentric cylindrical heat pipes forming a thermionic diode. Heat from the reactor fuel is radiated to the heat pipe emitter whose inner surface serves as the converter cathode. The second heat pipe is the collector and the converter anode. The heat from the reactor excites electrons in the emitter material and causes a flow of electrons across the interelectrode gap to the cooler collector. This generated current is supplied to an external load and returned to the cathode. The potential between the cathode and anode provides for a continuous flow of electrons as

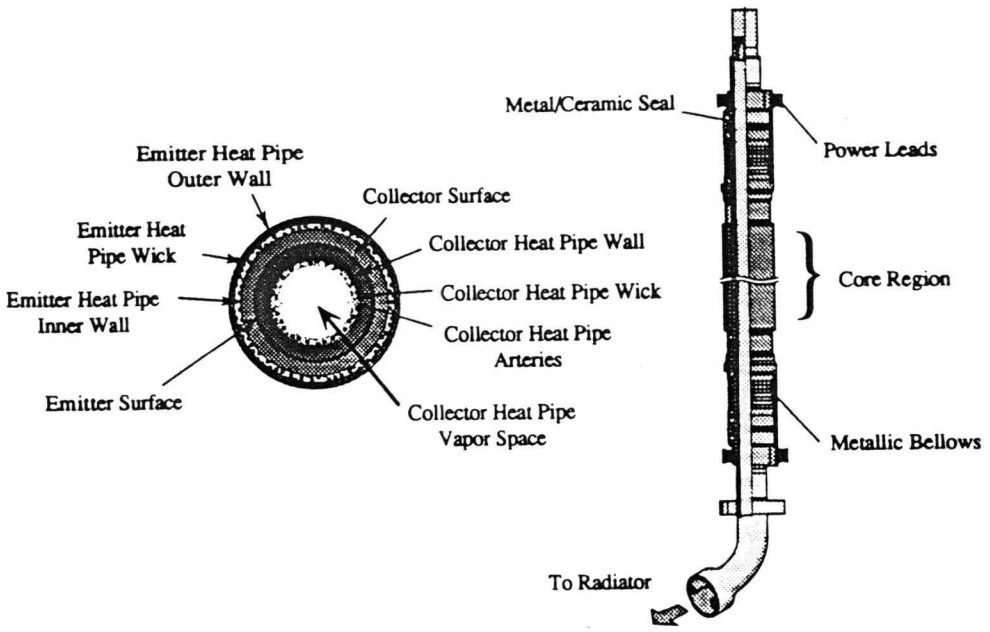

Figure 1.5. The Thermionic Heat Pipe Module (THPM) [10].

described. The collector heat pipe also transfers waste heat from the thermionic reactor to the radiator. The heat generated by the reactor can also provide propulsion. This is accomplished by passing hydrogen gas through the gap between the fuel and the THPMs. The expansion of the hot gas through a nozzle can provide direct thermal propulsion which, combined with electric propulsion, can produce a thrust sufficient to propel a spacecraft out of the earth's orbit and optimize a number of postulated missions [10].

The MOHTR, also a thermionic reactor, uses heat pipes to transfer waste heat from the converter collector to the radiator. The MOHTR uses a beryllium moderated thermionic reactor, zirconium hydride moderator rods, and stainless steel

- potassium heat pipes [11]. These are only a few of the many applications of heat pipes in space. A good discussion of space related heat pipe technology issues can be found in Merrigan [13].

Heat pipes have assumed a major role in the rejection of heat from space power systems. They continue to be investigated as the most reliable means of heat transfer for a large number of space applications. Further improvements in heat pipe technology will likely come from research and development within the space industry, and improvements in heat pipe design will have important implications for space power systems.

In the wake of the burgeoning space technology in the 1960's, terrestrial applications for heat pipes also began to emerge and saw rapid advancement during the early 1970's. Dunn and Reay attribute this growth largely to the "technological fallout" from the successful use of heat pipes in the space industry [14]. One of the first terrestrial uses for heat pipes, developed by engineers at RCA, was for cooling of transistor circuits in aircraft transmitters [7]. As electronic systems have become more powerful and generate much more heat, the use of heat pipes as heat sinks in electronic and integrated circuits has become common. Heat pipes have been successfully used as a means of removing heat from electrical systems ranging from electrical power generation and transmission lines to very high speed integrated circuits (VHSIC).

Perhaps the most celebrated terrestrial application of heat pipes is their use as "cryo-anchor stabilizers" on the trans-Alaskan oil pipeline. Here, heat pipes are

used to preserve the permafrost under the supports for the pipeline. The thawing of the permafrost creates engineering problems for the anchoring and supporting of structures due to shifting of the soil upon thawing. Nearly 100,000 ammonia-steel heat pipes are used to maintain the permafrost under the pipeline. These heat pipes were shown to be capable of removing up to 4 x 10^6 BTU/yr from the soil, allowing a 40 ft reduction in the length of the supporting piles. This has been one of the largest demonstrations of the reliability and cost effectiveness of heat pipes to date [15].

More recently, the concept of a *heat pipe thermodynamic cycle* and its applications have been examined. The heat pipe thermodynamic cycle operates from the varying vapor pressure of the heat pipe. By controlling the ability of the condenser section to reject heat, large cyclical pressure transients can be produced in the heat pipe. These pressure transients can in turn be used to drive a piston, thus creating a sort of "heat pipe engine" that can provide useful work [16]. Other major terrestrial applications of heat pipes include the deicing of highways, bridges, and airport runways [17-20], heat transfer and removal in solar energy collectors [21-23], air conditioning [24], distillation [25], automobile engine cooling and aftercooling [26-27], cooling in nuclear power plants [28-30], power plant waste heat recovery [31-32], solar cooking [33-34], geothermal energy [35], cooling of tandem mirror fusion reactors [36], lasers [37], and hand warmers [38].

This wide application of heat pipe technology has created a rich environment for research. The theory and operation of heat pipes has been studied extensively.

A sample of the available literature includes detailed analytical and computational studies of heat pipe fluid dynamics [39-50], operating characteristics and limits [51-59], design and construction [60-65], modeling [66-70], and the myriad of practical applications discussed above. Among the most comprehensive and often referenced sources on heat pipes are Dunn and Reay [14], and Chi [71].

1.3. Heat Pipe Theory

A heat pipe consists of a vessel lined with a wicking material containing a working fluid. Figure 1.6 shows the configuration of the basic heat pipe. Heat is added to one end of the heat pipe. The addition of heat to the evaporator section causes the working fluid to vaporize and creates a differential pressure between the evaporator and condenser sections of the heat pipe. This differential pressure

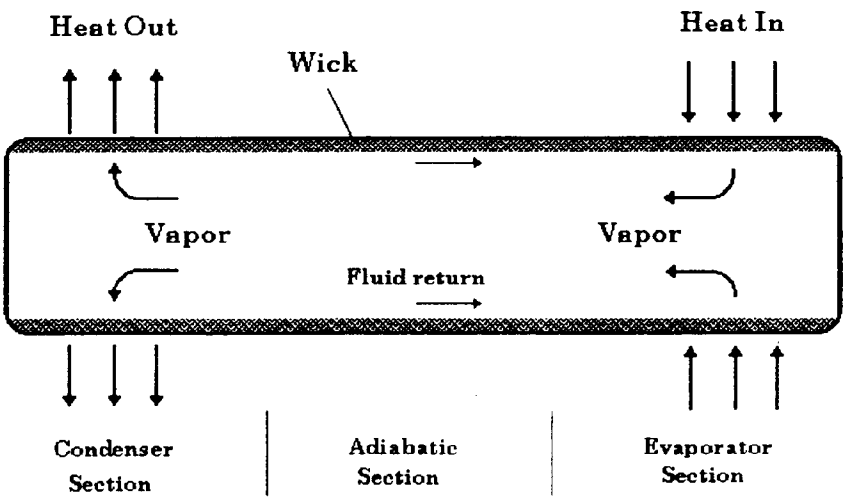

Figure 1.6. Diagram of the basic heat pipe

sustains the flow of the vapor from the evaporator section to the condenser section. At the opposite end of the heat pipe, heat is rejected to the surroundings, and the working fluid condenses. The condensing fluid is absorbed by the wick where capillary forces drive the fluid back to the evaporator section. This process will continue, within certain limits, indefinitely. The capillary forces are produced as a result of the pressure difference at the curved vapor - liquid interface. The characteristics of the wick, such as pore size and contact angle, can increase the maximum capillary pressure, allowing greater wicking rates.

A significant amount of energy is transferred in this process due to the latent heat of vaporization and condensation of the working fluid which accounts for the heat pipe's ability to achieve such a high thermal conductance. The two phase process also allows the heat pipe to transfer heat effectively with a small difference in temperature between the evaporator and condenser. The adiabatic section is not essential but will exist if there is an insulated length of the heat pipe separating the evaporator and condenser sections. Heat can be transferred from the condenser section to its surroundings by conduction, convection, or radiation.

Variations in the design of heat pipes include the use of a variety of working fluids, structural and wicking materials, and geometries. Water, alcohol, helium, acetone, ammonia, nitrogen, lithium, and liquid metals have all been used as working fluids in heat pipes. Most heat pipes are constructed of copper, aluminum, or stainless steel, but many space applications have used refractory metals such as titanium, niobium, and molybdenum. The material selected depends upon the

particular use of the heat pipe, the environment in which it operates, and the compatibility with the wick and working fluid. Wicking materials are generally of the wire mesh or sintered metal type, but other materials such as ceramic felts and metal foams have been used.

1.4. The Fabric Composite Heat Pipe

A simple way to reduce the cost of space power systems is to reduce the weight of the system. If such a system were to use heat pipes for heat rejection or temperature control, lighter heat pipes would be advantageous. A method for constructing a lightweight heat pipe for use in space has been suggested by Antoniak and Webb [72]. This method combines a woven ceramic fiber with a thin metal foil to form a lightweight, high strength, heat pipe. This design, referred to as a "fabric composite" heat pipe, is shown in Figure 1.7. The heat pipe vessel is constructed by forming a tube consisting of an outer layer of ceramic material and a thin metal liner. An internal layer of porous ceramic material serves as the heat pipe wick. The composite wall construction is shown in greater detail in Figure 1.8. The strength of the heat pipe -- its ability to withstand high internal pressures and external impingement -- is derived from the qualities of the ceramic material. Since the fabric is porous, however, a thin foil is used to contain the working fluid. The metal liner is not needed for structural strength and, therefore, can be made as thin as fabrication techniques will allow. Heat pipes of this design are very lightweight and have additional significant advantages [72-74].

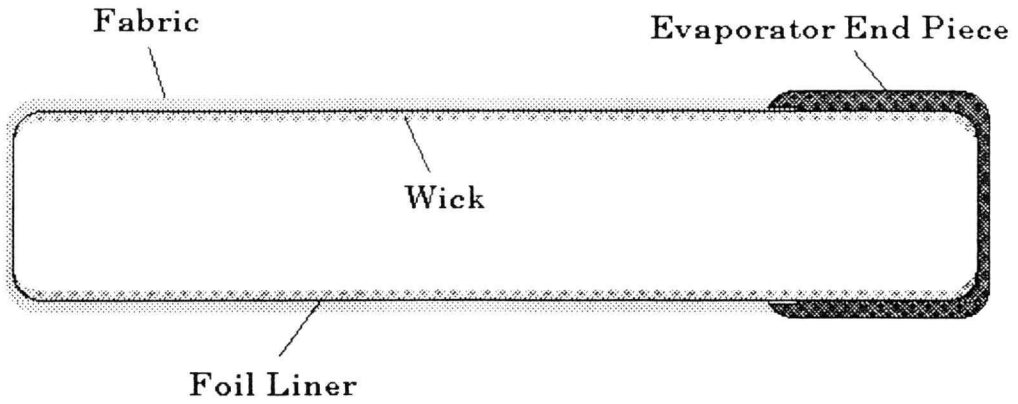

Figure 1.7. The Fabric Composite Heat Pipe

Aside from the drastic reduction in weight, the most significant improvement in heat pipe performance results from an increase in the effective emissivity of the condenser. This enhanced emissivity is due to both the emittance properties of the fabric and an increase in total surface area. Several ceramic fabrics have been shown to exhibit emissivities greater than that of stainless steel [75-76], and the weave and texture of the fabric creates an appreciable increase in the area of the radiating surface. These combined effects enable the heat pipe to reject heat (via radiation) much more efficiently. Thus, a much lighter fabric composite heat pipe can be constructed having a greater power capacity than conventional heat pipes.

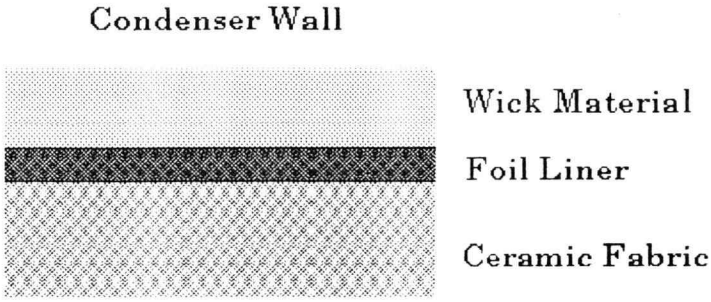

Figure 1.8. The Fabric Composite.

Other advantages of the fabric composite heat pipe design are promising. A great concern with the design of any space system is its ability to survive the impingement of micrometeoroids. Fabric composites can offer an advantage over conventional heat pipes in this area as well. Ceramic materials have been suggested as a type of shielding to micrometeoroids since layers of fabric can be expected to dissipate the energy of these projectiles while suffering less structural damage than a thin metal wall [73]. The flexible nature of the fabric composite would also allow for a very compact radiator comprised of compressed or rolled fabric composite heat pipes that would deploy upon start up in space. The ability of such heat pipes to deploy with the internal pressure generated upon start up was demonstrated in 1990 by Trujillo et al. [77].

A reduction in the weight and size of the system payload transforms into a significant reduction in the cost of launching a space power system. The potential advantages of fabric composite radiators should not be underestimated. The development of a small, lightweight, efficient heat rejection system was identified as a "*very* important design consideration" by the Committee on Advanced Nuclear Systems in 1983 [78]. The fabric composite design could conceivably improve upon the design criteria of low mass, low cost, efficiency, and survivability of space power systems.

1.5. Conclusion

The wealth of literature available attests to the wide interest and application of heat pipes. In particular, heat pipes have long played an important role in thermal management in space systems and continue to be the primary method proposed for waste heat rejection in space. Advances in the design of heat pipes for space radiators could have a tremendous impact on the viability and attractiveness of future space nuclear power systems. The present study has been undertaken to show, qualitatively, how the use of fabric composites can enhance the efficiency of heat pipe space radiators by reducing the weight of the radiator system while increasing its overall heat rejection capacity.

1.6. References

1. Gaugler, R.S., "Heat Transfer Device," U.S. Patent 2,350,348, June 6, 1944.

2. Grover, G.M., T.P. Cotter, and G.F Erickson, "Structures of Very High Thermal Conductance," *J. Appl. Phys.*, **35**, 1964, pp. 1990-1991.

3. Grover, G.M., J. Bohdansky, and C.A. Busse, "The Use of a New Heat Removal System in Space Thermionic Power Supplies," European Atomic Energy Community, EURATOM Report EUR 229.e, 1965.

4. Reid, R.S., M.A. Merrigan, and J.T. Sena, "Review of Liquid Metal Heat Pipe Work at Los Alamos," *Proc. 8th Symposium on Space Nuclear Power Systems*, AIP CONF-910116, Albuquerque, NM, 1991.

5. Cotter, T.P., "Theory of Heat Pipes," Los Alamos Scientific Laboratory Report LA-3246-MS, February 1965.

6. Deverall, J.E. and E.W. Salmi, "Heat Pipe Performance in a Zero Gravity Field," *J. of Spacecraft and Rockets,* **4**, 1967, pp. 1556-1557.

7. Brennan, P.J and E.J. Kroliczek, *Heat Pipe Design Handbook*, NTIS N81-70112, B&K Engineering Inc., Towson, MD, June 1979.

8. Ranken, W.A., "Heat Pipe Development for the SPAR Space Power System," *IVth International Heat Pipe Conference,* London, UK, September 7-10, 1981.

9. Truscello, V.C. and L.L. Rutger, "The SP-100 Power System," *Proc. 9th Symposium on Space Nuclear Power Systems*, AIP-CONF 920104, Albuquerque, NM, January 12-16, 1992.

10. Jacox, M.G and A.C. Zuppero, "The SEHPTR Stage: A Thermionic Combined Power and Propulsion Technology for Space Application," *Proc. Nuclear Technologies for Space Exploration 1992*, Jackson Hole, WY, August 16-19, 1992.

11. Merrigan, M.A. and V.L. Trujillo, "Moderated Heat pipe Thermionic Reactor (MOHTR) Module Development and Test," *Proc. 9th Symposium on Space Nuclear Power Systems*, AIP CONF-920104, Albuquerque, NM, January 12-16, 1992.

12. "Thermionic Heat Pipe Module," *Near Term Technology for Nuclear Power and Propulsion Systems*, Thermacore Inc./INEL, August 16, 1992.

13. Merrigan, M.A., "Heat Pipe Technology Issues," *Space Nuclear Power Systems*, M.S. El-Genk and M.D. Hoover, ed., Orbit Book Co., Malabar, FL, 1985.

14. Dunn, P.D. and D.A. Reay, *Heat Pipes 3rd Ed.*, Pergamon Press, Oxford, England, 1982.

15. Waters, E.D., "Arctic Tundra Kept Frozen by Heat Pipes," *The Oil and Gas Journal*, August 26, 1974, pp. 122-125.

16. Kobayashi, Y., "Heat Pipe Thermodynamic Cycle and Its Applications," *J. Solar Energy Engineering*, **107**, May 1985, pp. 153-159.

17. Bienert, W.B., "Snow and Ice Removal From Pavements Using Stored Earth Energy," Final Report, No. FHWA-RD-75-6, Dynatherm Corp., Cockeysville, MD, May 1974.

18. Ferrara, A.A. and R. Haslett, "Prevention of Preferential Bridge Icing Using Heat Pipes," Final Report FHWA_RD_75-111, Grumman Aerospace Corp., Bethpage, New York, July 1975.

19. Pravda, M.F., "Heating Systems for Airport Pavement Snow, Slush, and Ice Control," Final Report, FAA-RD-75-139, Dynatherm Corp., Cockeysville, MD, July 1975.

20. Tanaka, O., H. Yamakage, T. Ogushi, M. Marakami, and Y. Tanaka, "Snow Melting Using Heat Pipes," *IVth International Heat Pipe Conference*, London, UK, September 7-10, 1981.

21. Ribot, J. and R.D. McConnell, "Testing and Analysis of a Heat Pipe Solar Collector," *J. of Solar Energy Engineering*, **105**, November 1983, pp. 440-445.

22. Saatci, A.M., I.A. Olwi, and R.R. Al-Hindi, "Passive Transport of Solar Energy Downward By Heat Pipes," *Energy*, **14**, July 1989, pp.383-392.

23. Adkins, D.R. "Experiments on Bench-Scale Heat Pipe Solar Receivers," *Proc. 8th Symposium on Space Nuclear Power Systems*, AIP CONF-910116, Albuquerque, NM, 1991.

24. "Passive Cooling and Heating with Heat Pipes," *Energy Engineering*, **81**, No. 6, 1984, pp.71-73.

25. "Space Age Distillation Using a Heat Pipe," *Chemical Engineer*, **444**, January 1988, p. 19.

26. "Heat Pipe Refrigerator," *Automotive Engineering*, **96,** October 1988, pp. 26-28.

27. Bak, D.J., "Self-Contained Aftercooler Increases Engine's Horsepower," *Design News*, June 2, 1986, p.41.

28. "Heat Pipes Have Power to Cut Nuclear Plant Costs," *Design News*, June 2, 1986, p. 41.

29. "NNC Installs Novel Type Heat Pipe at Nuclear Power Station," *Energy Conversion and Management,* **26**, 1986, pp. I-II.

30. "Novel Heat Pipes Improve Nuclear Cooling Problem," *Process Engineering,* **67**, No. 1, Feb. 1986, p. 17.

31. Holzhauer, R., "Waste Heat Recovery Equipment," *Plant Engineering*, **41**, January 8, 1987, pp. 58-62.

32. "Heat Pipe Array Gathers Waste Heat in Cooling," *Energy Engineering*, **84**, 1987, pp. 64-65.

33. Walker, J., "Gismos That Apply Non-Obvious Physical Principles to the Enjoyment of Cooking," *Scientific American*, **250**, June 1984, pp.146-153.

34. Khalifa, A.M.A., M.M.A. Thaha, and A. Manaa, "A Split-System Solar Cooker With Heat Pipes," *Energy Conversion and Management,* **26**, 1986, pp.259-264.

35. "Turning Old Oil Wells Into Power Sources," *New Scientist*, October 3, 1985, p. 34.

36. Schwertz, N.L. and M.A. Hoffman, "A Heat Pipe Concept For Cooling A Liquid-Pool Blanket of A Tandem Mirror Fusion Reactor," *Fusion*, **4** Nov. 1983, pp. 479-490.

37. Rieger, H., "Stimulated Raman Scattering in Lead Vapor Heat Pipe For Tunable and Narrow-Linewidth XeCl Excimer Laser," *J. of Quantum Electronics*, **25**, May 1989, pp. 913-916.

38. Faghri, A., D.B. Reynolds, and P. Faghri, "Heat Pipes for Hands," *Mechanical Engineering*, June 1989, pp. 70-74.

39. Issacci, F., I. Catton, and N.M. Ghoniem, "Vapor Dynamics of Heat Pipe Start-Up," *J. Heat Transfer*, **113**, Nov. 1991, pp. 985-994.

40. Lock, G.S.H. and J.D. Kirchner, "Some Characteristics of the Inclined, Closed Tube Thermosyphon Under Low Rayleigh Number Conditions," *Int. J. of Heat and Mass Transfer*, **35**, 1992, pp.165-173.

41. Faghri, A., M.M. Chen, and M. Morgan, "Heat Transfer Characteristics in Two-Phase Closed Conventional and Concentric Annular Thermosyphons," *J. of Heat Transfer*, **111**, Aug. 1989, pp. 611-618.

42. Roche, G.L., F. Issacci, and I Catton, "Liquid Phase Transient Behavior of a High Temperature Heat Pipe," *Proc. 7th Symposium on Space Nuclear Power Systems*, AIP CONF-900901, Albuquerque, NM, Jan. 7-10 1990.

43. Richardson, J.T., S.A. Paripatyadar, and J.C. Shen, "Dynamics of A Sodium Heat Pipe Reforming Reactor," *AIChE Journal*, 34, may 1988, pp. 743-752.

44. Faghri, A. and S. Thomas, "Performance Characteristics of a Concentric Annular Heat Pipe: Part I - Experimental Prediction and Analysis of the Capillary Limit," *J. of Heat Transfer*, **111**, Nov. 1989, pp. 844-850.

45. Faghri, A., "Performance Characteristics of a Concentric Annular Heat Pipe: Part II - Vapor Flow Analysis," *J. of Heat Transfer*, **111**, Nov. 1989, pp. 851-857.

46. Faghri, A., M. Buchko, and Y. Cao, "A Study of High Temperature Heat Pipes With Multiple Heat Sources and Sinks: Part II - Analysis of Continuum Transient and Steady State Experimental Data With Numerical Predictions," *J. of Heat Transfer*, **113**, Nov. 1991, pp. 1010-1016.

47. Dobran, F., "Suppression of the Sonic Heat Transfer Limit in High Temperature Heat Pipes," *J. of Heat Transfer*, **111**, Aug. 1989, pp. 605-610.

48. Chang, W.S. and J.S. Yu, "A note on the Gas Distribution in a Cylindrical Gas-Loaded Heat Pipe," *J. of Heat Transfer*, **112**, Aug. 1990, pp. 779-781.

49. Libera, J. and D. Poulikakos, "Parallel-Flow and Counterflow Conjugate Convection in a Vertical Heat Pipe," *J. of Heat Transfer*, **112**, Aug. 1990, pp. 797-802.

50. Peterson, P.F. and C.L. Tien, "Mixed Double-Diffusive Convection in Gas-Loaded Heat Pipes," *J. of Heat Transfer*, **112**, Feb. 1990, pp. 79-83.

51. Woloshun, K.A., J.T. Sena, E.K. Keddy, and M.A. Merrigan, "Radial Heat Flux Limits in Potassium Heat Pipes: An Experimental and Analytical Investigation," *Proc. 7th Symposium on Space Nuclear Power Systems*, AIP CONF-900901, Albuquerque, NM, Jan. 7-10 1990.

52. Stroes, G., D. Fricker, F. Issacci, and I. Catton, "Studies of Wick Dry-Out and Re-Wet," *Proc. 7th Symposium on Space Nuclear Power Systems*, AIP CONF-900901, Albuquerque, NM, Jan. 7-10 1990.

53. Jang, J. H., "Cool-Down and Frozen Start-Up Behavior of a Grooved Water Heat Pipe," NASA Contractor Report 187053, December, 1990.

54. Sena, J.T. and M.A. Merrigan, "Niobium 1% Zirconium/Potassium and Titanium/Potassium Life-Test Heat Pipe Design and Testing," Proc. 7th

55. Reinarts, T.R. and F.R. Best, "Water Heat Pipe Frozen and Non-Frozen Startup and Shutdown Transients with Internal Measurements and Visual Observations," Proc. 7th

56. Phillips, J.R., L.C. Chow, and W.L. Grosshandler, "Thermal Conductivity of Metal Cloth Heat Pipe Wicks," *J. of Heat Transfer*, **109**, Aug. 1987, pp. 775-781.

57. Ponnappan, R., J.E. Beam, and E.T. Mahefkey, "A Liquid Metal Variable Conductance Heat Pipe for Space Radiators," *Proc. 7th Symposium on Space Nuclear Power Systems*, AIP CONF-900901, Albuquerque, NM, Jan. 7-10 1990.

58. Jang, J.H., W.P. Lucas, K.W. Baker, and A.J. Juhasz, "Preliminary Report on Copper-Water Heat Pipe Tests at NASA Lewis Research Center," *Proc. 7th Symposium on Space Nuclear Power Systems*, AIP CONF-900901, Albuquerque, NM, Jan. 7-10 1990.

59. Holtz, R.E., "Testing of a Sodium Heat Pipe," *Proc. 8th Symposium on Space Nuclear Power Systems*, AIP CONF-910116, Albuquerque, NM, 1991.

60. Miskolczy, G. and C.C.M. lee, "Heat Pipe Design for Sheath Insulator Reactor Test," *Proc. 8th Symposium on Space Nuclear Power Systems*, AIP CONF-910116, Albuquerque, NM, 1991.

61. Pruzan, D.A., L.K. Klingensmith, K.E. Torrance, and C.T. Avedisian, "Design of High-Performance Sintered-Wick Heat Pipes," *Int. J. Heat Mass Transfer*, **34**, 1991, pp. 1417-1427.

62. Horner-Richardson, K., J.R. Hartenstine, D.M. Ernst, and M.G. Jacox, "Fabrication and Testing of Thermionic Heat Pipe Module for Space Nuclear Power Systems," *27th IECEC,* San Diego, CA, Aug. 1992.

63. Anand, D.K., A.Z. Dybbs, and R.E. Jenkins, "Effects of Condenser Parameters on Heat Pipe Optimization," *Journal of Spacecraft and Rockets,* May 1967, pp.695-696.

64. Edelstein, F.E. and R. Kosson, "A High Capacity Re-entrant Groove Heat Pipe for Cryogenic and Room Temperature Space Applications," *Cryogenics*, 32, 1992, pp. 167-172.

65. Seshan, S. and D. Vijayalakshmi, "Heat Pipes - Concepts, Materials, and Applications," *Energy Conversion Management*, 26, 1986, pp. 1-9.

66. Chow, L.C. and J. Zhong, "Startup of Sodium Heat Pipes From Room Temperature," *Proc. 8th Symposium on Space Nuclear Power Systems*, AIP CONF-910116, Albuquerque, NM, 1991.

67. Faghri, A. and M. Buchko, "An Experimental and Numerical Analysis of Low-Temperature Heat Pipes With Multiple Heat Sources," *J. of Heat Transfer,* **113**, Aug. 1991, pp. 728-7344.

68. Rao, D.V., M.S. El-Genk, and A.J. Juhasz, "Transient Model of High Temperature Heat Pipes," *Proc. 7th Symposium on Space Nuclear Power Systems*, AIP CONF-900901, Albuquerque, NM, Jan. 7-10 1990.

69. Tournier, J.-M. and M.S. El-Genk, "HPTAM Heat Pipe Transient Analysis Model: An Analysis of Water Heat Pipes," *Proc. 9th Symposium on Space Nuclear Power Systems*, AIP CONF-920104, Albuquerque, NM, January 12-16, 1992.

70. Babin, B.R. and G.P Peterson, "Experimental Investigation of a Flexible Bellows Heat Pipe for Cooling Discrete Heat Sources," J. of Heat Transfer, 112, Aug. 1990, pp. 602-607.

71. Chi, S.W., *Heat Pipe Theory and Practice: A Sourcebook*, Hemisphere, Washington, 1976.

72. Antoniak, Z.I. and B.J. Webb, "Construction and Testing of Fabric Heat Pipe Components for Space Nuclear Power Systems, *Proc. 6th Symposium on Space Nuclear Power Systems*, Albuquerque, NM, January 8-12, 1989.

73. Antoniak, Z.I, W.J. Krotiuk, B.J. Webb, J.T. Prater, and J. M. Bates, *Fabric Space Radiators*, PNL-6458, Pacific Northwest Laboratory, Richland, WA, 1988.

74. Antoniak, Z.I. and B.J. Webb, "Construction and Testing of Advanced Ceramic Fabric Radiator Components to 1000 K", *Proc. 7th Symposium on Space Nuclear Power Systems*, CONF-900901, Albuquerque, NM, 1990.

75. Antoniak, Z.I, B.J. Webb, J.M. Bates, and M.F. Cooper, "Construction and Testing of Ceramic Fabric Heat Pipe With Water Working Fluid," *Proc. 8th Symposium on Space Nuclear Power Systems*, CONF-910116, Albuquerque, NM, 1991.

76. Klein, A.C., Z. Gulsha-Ara, W.C. Kiestler, R.D. Snuggerud, and T.S. Marks, "Fabric Composite Heat Pipe Technology Development," *Proc. 10th Symposium on Space Nuclear Power Systems*, Albuquerque, NM, Jan. 10-14, 1993.

77. Trujillo, V.L., E.S. Keddy, and M.A. Merrigan, "High Temperature, Deployable, Membrane Heat Pipe Radiator Element: Demonstration and Status," *Proc. 7th Symposium on Space Nuclear Power Systems*, CONF-900901, Albuquerque, NM, 1990.

78. *Advanced Nuclear Systems for Portable Power in Space*, Report prepared by the Committee on Advanced Nuclear Systems, Energy Engineering Board, Commission on Engineering and Technical Systems, National Research Council, National Academy Press, Washington D.C., 1983.

CHAPTER 2. THE HEAT PIPE TEST FACILITY

2.1. Introduction

In order to evaluate the performance of fabric composite heat pipes, a test facility has been designed and built to accommodate a variety of heat pipe designs. The Heat Pipe Test Facility (HPTF) allows for the operation and evaluation of single or multiple heat pipes, in a vacuum, at low temperatures. This chapter provides a detailed description of the HPTF and the heat pipe testing principles and procedures.

2.2. Test Facility

2.2.1. Physical Description

The Heat Pipe Test Facility consists of two mild steel concentric cylinders (15 and 25 cm ID) welded together to form an outer cooling jacket and an inner vacuum chamber. The inner vacuum chamber is 101 cm (40 in.) deep. The cooling jacket is insulated with 5 cm (2 in.) of highly compressed, rigid fiberglass insulation. A recirculating bath chiller is used to circulate a 50% aqueous ethylene-glycol coolant, at temperatures as low as -20°C, through the cooling jacket. The inner cylinder is smooth and painted flat black to allow for maximum radiation heat transfer. The test chamber is sealed by a teflon end piece with an o-ring seal. The teflon end piece also contains leads for heater power input and thermocouples,

the heat pipe evacuation and charging line, and a tube for drawing a vacuum on the test chamber. The evacuation and charging line is fitted with a DC pressure transducer for monitoring the heat pipe operating pressure and has a four-way valve that can be positioned for evacuation of the heat pipe, charging the working fluid, or shutoff. A schematic diagram of this facility is shown in Figure 2.1.

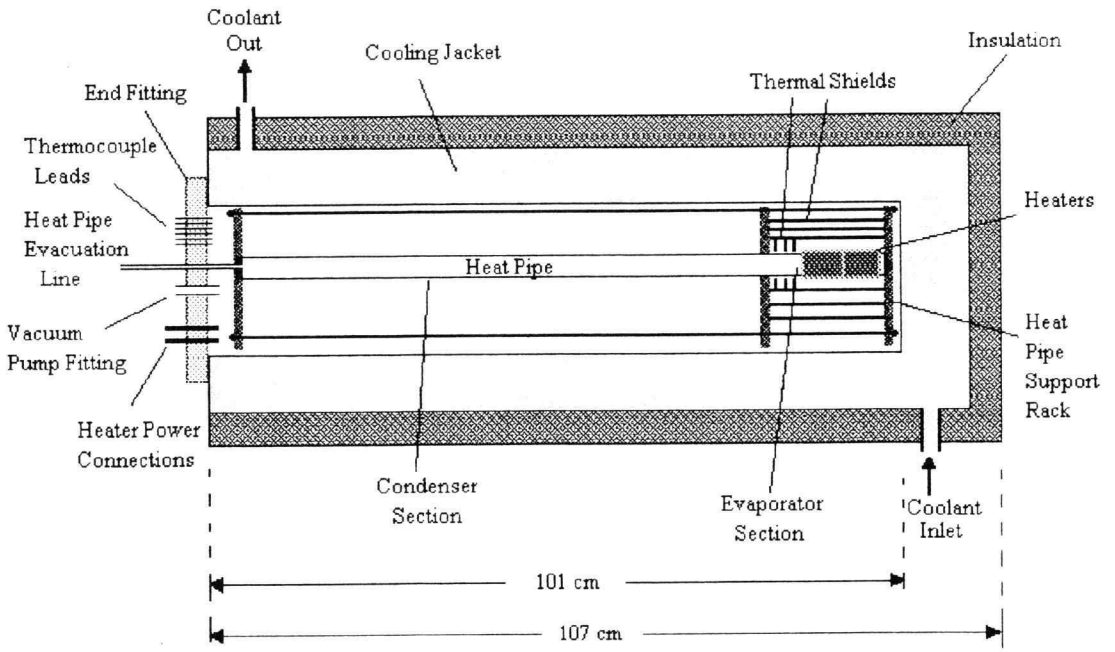

Figure 2.1. The Heat Pipe Test Facility.

A mounting rack was designed to hold the heat pipe in position while testing and to provide shielding for all forms of heat transfer other than radiation from the heat pipe condenser section. The mounting rack can be seen in Figure 2.1 and is shown in greater detail in Figure 2.2. The mounting rack consists of three teflon

disks connected by stainless steel rods. The condenser end disk provides support for the heat pipe and limits the amount of radiation heat transfer in the axial direction. The other two disks help to form the thermal radiation shield around the evaporator end of the heat pipe. Ideally, all of the power input into the heat pipe would be rejected by radiation from the condenser section; however, a small amount of energy is lost by heat transfer from the evaporator section and from the heaters themselves. The purpose of the evaporator shield is to minimize the amount of heat lost through conduction and radiation to the cooling jacket from the

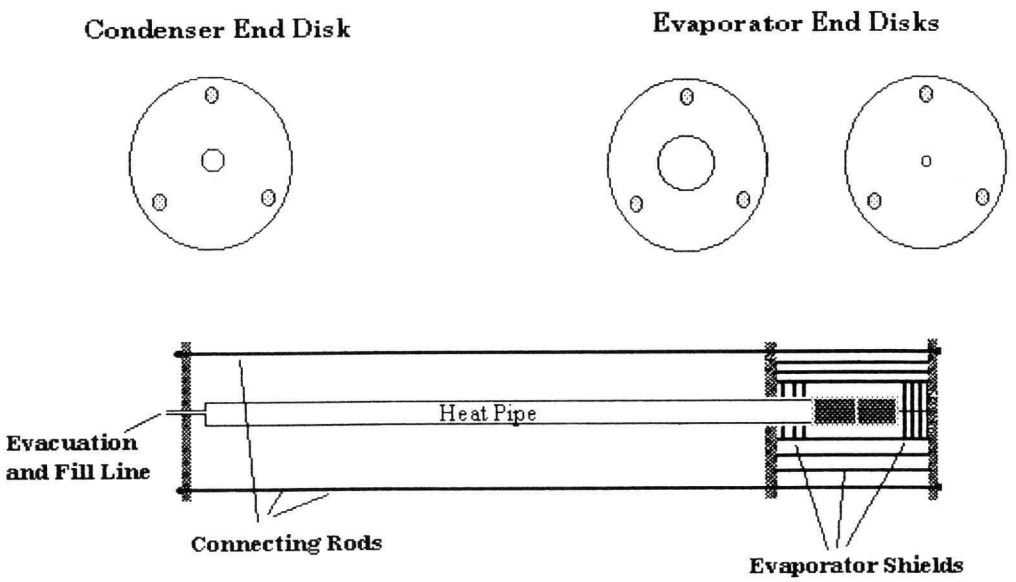

Figure 2.2. Heat Pipe Mounting Rack.

evaporator and heaters. The evaporator shield consists of the two teflon disks and stainless steel plates for axial shielding and four concentric stainless steel cylinders for radial shielding. The shield was shown to be fairly efficient, allowing less than 10% heat loss from the evaporator end.

2.2.2. Instrumentation.

The HPTF is cooled by a PolyScience Model 900 constant temperature circulating bath. This chiller circulates coolant between the HPTF cooling jacket and a 5 liter reservoir. A dual speed centrifugal pump provides flow of up to 15 l/min, depending on the coolant viscosity and system head. Under the conditions for the tests conducted, slow pump speed corresponded to a flow rate of approximately 3.8 l/min (1 gpm), and fast speed provided approximately 7.6 l/min (2 gpm). The chiller is rated at 240 W at -20°C, but the range of the constant temperature controller is -15°C to 100°C.

Pressure in the vacuum chamber is monitored using a standard bellows type gauge. The gauge measures pressure over a range of -100 to 200 kPa (30 in Hg vac. to 30 psig). The vacuum chamber pressure is not monitored or recorded by the data acquisition system. It must be checked visually periodically during testing to verify the vacuum in the test chamber. If the pressure rises in the test chamber, the vacuum can be easily redrawn with a vacuum pump without adverse effect on the heat pipe or heat pipe tests. This was generally not required, however, as the facility held a vacuum quite well.

The volumetric flow rate of the coolant is measured by an Omega acrylic rotameter. The flow meter uses a guided stainless steel float to measure the flow rate from 0 to 5 gpm. The rotameter is accurate to within 4% of full scale but is calibrated for fluids having a specific gravity equal to 1.0. Thus, the uncertainty in the properties of the aqueous ethylene-glycol mix contributes to an appreciable overall uncertainty in the measurement of the coolant flow rate. The consequences of this uncertainty are discussed in Section 2.2.3.

An Omega PX300-500G-V 10 volt DC pressure transducer is used to continuously monitor the pressure in the heat pipe. The pressure transducer operates over a range of 0 to 500 psi and provides a linear signal from 0 to 30 mv. The output is coupled to the data acquisition system through an Omega signal amplifier which has a maximum output voltage of $\pm$ 9 VDC. The gain of the amplifier (10x, 100x, or 1000x) is set to provide a signal within the $\pm$5 VDC analog input range of the data acquisition system. The data acquisition system is described in more detail in Section 2.3.

Heat is provided to the heat pipe evaporator end by two 7.6 cm (3 in) band heaters. The power to the heaters is controlled using a voltage rheostat. The heater voltage is adjustable from 0 to 120 VAC. An ammeter in line with the heater wire provides a measurement of the current to the heaters. The voltage and current are used to determine the power delivered to the heat pipe.

Chromel-Alumel (K-type) thermocouples are used to measure the temperatures associated with the heat pipe and HPTF. The thermocouples monitor

the temperature of the inlet and outlet coolant as well as the surface temperature at various axial positions on the heat pipe, vacuum chamber walls, and radiation shields. The thermocouples and their configuration are discussed in Section 2.3.2.

2.2.3. Theory.

The HPTF was designed to simulate the space environment as nearly as possible. Thus it is designed to provide a cold, black surrounding for the heat pipe. It is assumed that heat transfer from the heat pipe to the vacuum chamber wall is accomplished solely by radiation with the configuration factor for infinite concentric cylinders. These assumptions are used in evaluating the radiation heat transfer in the test chamber. The design of the heat pipe mounting rack ensures that, in a vacuum, the only mode of heat transfer is by radiation. Since there is very little contact between the heat pipe and the teflon support disks and since teflon has very poor thermal conductivity, heat transfer by conduction is negligible. Additionally, the infinite concentric cylinder approximation for the configuration factor between the heat pipe and the vacuum chamber wall is unity, so the equation for radiation heat transfer between the heat pipe and the cooling jacket is given by

$$Q = \frac{\sigma A_{hp}(T_{hp}^4 - T_{vc}^4)}{\frac{1}{\varepsilon_{hp}} + \frac{1-\varepsilon_{vc}}{\varepsilon_{vc}}\left(\frac{r_{hp}}{r_{vc}}\right)^2} \qquad (2.1)$$

where Q is the heat transferred by radiation from the heat pipe condenser section to the vacuum chamber walls.

The power, Q, can be determined either by performing an energy balance across the HPTF cooling jacket as in Equation 2.2, or by direct measurement of the

$$\dot{Q} = \dot{m} c_p (T_{out} - T_{in}) \tag{2.2}$$

power input (corrected for heat loss from the evaporator section). The energy balance, or calorimetric method, while useful for verifying proper operation of the HPTF, was far too inaccurate for evaluating the radiative properties of the heat pipes. This inaccuracy is due to the large fractional uncertainties in the mass flow rate and the temperature change across the HPTF, ΔT_{HPTF}. For the range of power levels observed in the heat pipe tests, the fractional uncertainty in the flow rate and ΔT_{HPTF} were about 20% and 140%, respectively. Therefore, a direct measurement of the power to the heaters was used in evaluating the heat pipe performance. The amount of power supplied to the heaters is determined by measuring the voltage and current delivered to the heaters. The method for measuring the power input and for calculating heat loss from the evaporator is discussed in detail in Chapter 4. In order to determine the radiant properties of the fabric composite, Equation 2.1 is solved for the emissivity of the heat pipe, ε_{hp}.

2.3. Data Acquisition

2.3.1. The Data Acquisition System.

An 8088 processor-based personal computer and an Omega DAS-8 analog/digital interface board are used to provide continuous monitoring and logging of the heat pipe and HPTF parameters. The DAS-8 system contains eight single ended, analog input channels and uses a 12-bit, successive approximation A/D converter with a nominal conversion time of 25 μsec.

Two Omega Model EXP-16 Analog Input Multiplexers are used to provide up to 32 channels of monitoring on one DAS-8 channel. One EXP-16 is used to measure temperatures, and the other is used to measure the heat pipe pressure. The multiplexer boards are connected using a 37 pin D type male plug. The EXP-16 gain setting is adjustable from 0.5x to 1000x. A dip switch on the board selects gains of 0.5, 1, 2, 10, 50, 100, 200, or 1000. A higher gain setting reduces noise and fluctuation in the thermocouple signal but limits the maximum measurable temperature. Conversely, lower gain settings increase the measurable temperature range but result in greater fluctuation in the signal. A gain of 1000 limited the maximum measurable temperature to less than about 128°C, and a gain of 200 resulted in a fluctuation in the temperature signal of ± 6°C. Therefore, a 330 ohm resistor was added to the gain circuitry in order to provide a gain of 606. This gain setting allowed temperature measurements up to 225°C while reducing the temperature signal oscillation to about ± 1°C. It is necessary to use separate

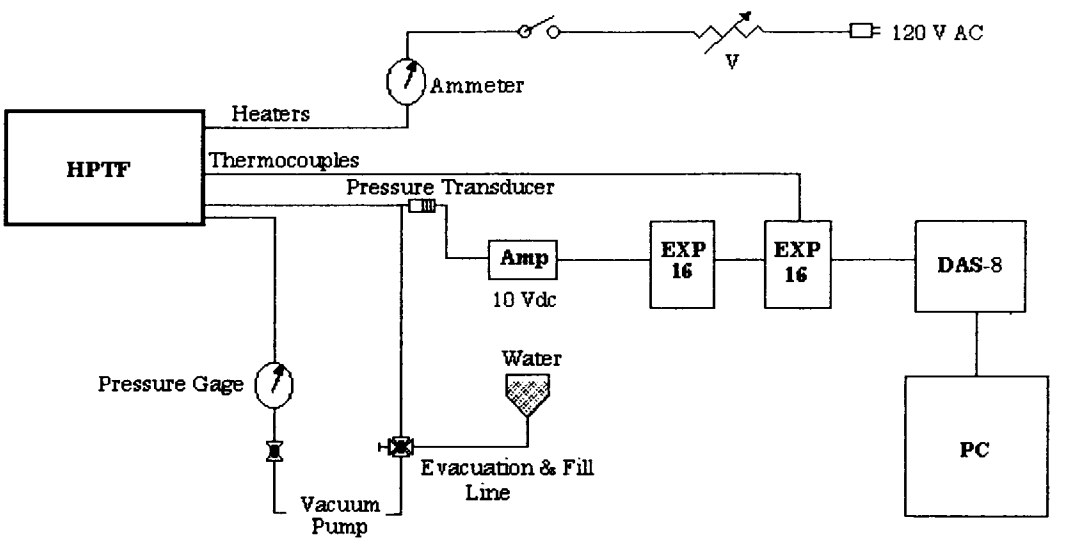

Figure 2.3. Schematic diagram of heat pipe test apparatus.

multiplexers for temperature and pressure because the required gain settings are different. A gain of 50 was used for the heat pipe pressure measurement. A total of 32 channels are available, but only 16 were used during the heat pipe tests. Fifteen channels were used to measure the temperatures, and one channel was used to monitor the heat pipe pressure. Figure 2.3. is a schematic diagram of the complete test apparatus.

2.3.2. Thermocouples.

All temperatures were measured using Chromel - Alumel (K-type) thermocouples. These thermocouples are capable of measuring temperatures from

-270°C to 1370°C. As discussed above, the upper and lower limits on the measurable temperature response, however, are a function of the multiplexer gain, since the input analog voltage is limited to ± 5 VDC. The EXP-16 provides a cold junction compensation voltage which is used by the data acquisition software in calculating measured temperatures. A total of 15 channels of the #1 EXP-16 were used for temperature measurements. Table 2.1 summarizes the location of the thermocouples assigned to each of the EXP-16 channels. Thermocouples 3 through 9 were placed approximately 10 cm apart along the condenser section to verify the nearly isothermal conditions expected along the condenser and to provide the temperature measurements used to calculate the emissivity of the heat pipe. For the fabric composite tests, thermocouples 3 and 9 were placed underneath the fabric.

Table 2.1. Thermocouple Locations

EXP-16 Channel #	Location of Thermocouple
0,1	Heat pipe evaporator
2	External evaporator radiation shield
3-9	Heat pipe condenser surface
10-12	Vacuum chamber walls
13	Coolant inlet
14	Coolant outlet

2.3.3. Data Acquisition Software.

The DAS-8 is controlled using programs written in Microsoft QuickBASIC. BASIC(A) can also be used; however, QuickBASIC is capable of faster data sampling rates and has a convenient, user-friendly working environment. The data acquisition code is called QBHPR.BAS and is listed in Appendix A. The program accomplishes the following tasks:

1. Initializes the DAS-8 and loads the thermocouple look up table.
2. Measures temperature for cold junction compensation.
3. Measures the voltages of all thermocouples on #1 EXP-16.
4. Converts, corrects, and linearizes thermocouple volts to temp. in °C.
5. Measures the output voltage of pressure transducer on #2 EXP-16.
6. Converts and corrects to measure pressure in kPa.
7. Calculates Q based on calorimetric.
8. Estimates ε_{hp} based on calorimetric.
9. Displays output.
10. Writes the output to a data file.

The DAS-8 software requires a special input and output (I/O) driver routine, "DAS8.BIN," which allows several of the DAS-8 functions to be called using the BASIC statement CALL. When running in the QuickBASIC environment a Quick Library must be created to allow the program to use the DAS8 routines. A batch file was written to execute QuickBASIC, create the Quick Library, and run the data acquisition program with one command. This routine, HPRUN.BAT, is as follows:

```
QB /AH /RUN QBHPR.BAS /L DAS8.QLB
```

With the batch file, the data acquisition program is started by simply typing "HPRUN."

The code performs the data acquisition and A/D conversion procedures by referencing the DAS8 Quick Library. Each of these procedures is associated with a particular mode of the DAS8 routine. Twenty two modes are available, but only a few were required for the data acquisition associated with the heat pipe tests. A description of the applicable modes is given in Table 2.2.

Table 2.2. Summary of DAS8 Modes

MODE	FUNCTIONAL DESCRIPTION
0	Initialize the DAS-8, set base address
1	Set channel scan limits
4	Perform single A/D conversion
14	Write digital outputs

The values of Q and ε_{hp} computed by the program are not actually used in the evaluation of the heat pipe performance. Since these values are calculated using the calorimetric procedure, they provide only a rough estimate of the radiation heat transfer occurring in the HPTF. They were included in the program to give a real-time estimate of the proper operation of the heat pipe. Thus, each time the data is written to the output file, the current estimate of Q and ε_{hp} are displayed. The calculation is based on the data averaged over the last recording interval. The data recording rate is adjusted by setting the upper integer value, J_{max}, for the data sampling loop (line 602). The data is then taken and displayed on the screen for each step of the sampling loop, but it is not written to the output file until the loop

count reaches J_{max}. While in the sampling loop, the measured values are averaged so that the recorded values are averaged over the entire data recording interval. This data averaging is a software fix to the problem with the thermocouple voltage fluctuations described in Section 2.3.1.

2.4. Test Procedures

The HPTF is designed to accommodate a variety of heat pipe designs, and procedures will vary somewhat for the testing of different heat pipes. Special considerations and precautions must be taken when handling and testing a lightweight fabric composite heat pipe because the heat pipe is not rigid until pressurized. These heat pipes must be handled with great care to prevent bending or crushing the liner. Once the heat pipe is loaded into the HPTF, a vacuum must be drawn on the test chamber prior to evacuating the heat pipe to prevent collapsing the fabric composite condenser. The three heat pipes tested to date were relatively rigid, and the liners were sufficiently thick to preclude any of these problems. Nonetheless, the procedure for testing the fabric composite heat pipes assumed a lightweight design, so that one procedure could be used to test any fabric composite heat pipe. For example, the HPTF vacuum chamber was always evacuated before the heat pipe. The complete heat pipe test procedure is provided in Appendix B.

2.5. Conclusion

The Heat Pipe Test Facility provides an excellent means for testing the performance of heat pipes for space power applications. The conditions simulated by the vacuum chamber are modeled after the space environment. The presence of a vacuum, combined with the design of the heat pipe mounting rack and evaporator shields, allow the radiative properties of the heat pipe to be properly evaluated. The data acquisition system provides for the continuous monitoring of heat pipe parameters during transient and steady state operations. Hence, the HPTF is suitable for testing heat pipe startup, shutdown, and transient behavior; evaluating operating limits; or performing life tests. The HPTF was successfully used to compare the performance of conventional and fabric composite heat pipes.

2.6. References

1. Incropera, F.P., and D.P. Dewitt, *Fundamentals of Heat and Mass Transfer*, 2nd Ed., John Wiley & Sons, New York, 1985.

2. Siegel, R., and J.R. Howell, *Thermal Radiation Heat Transfer*, 2nd Ed., Hemisphere, New York, 1981.

3. Taylor, J.R., *An Introduction to Error Analysis: The Study of Uncertainties in Physical Measurements*, University Science Books, Mill Valley, CA, 1982.

4. *DAS-8PGA A/D Interface Board Operator's Manual*, Omega Engineering Inc., Stamford, CT, 1989.

5. *MODEL EXP-16 Analog Input Multiplexer Operator's Manual*, Omega Engineering Inc., Stamford, CT, 1988.

6. *Microsoft QuickBASIC*, Microsoft Corporation, Redmond, WA, 1990.

7. Marks, T.S., "An Investigation of Fabric Composite Heat Pipe Feasibility Issues," M.S. Thesis, Oregon State University, Corvallis, OR, 1992.

CHAPTER 3. HEAT PIPE DESIGN AND CONSTRUCTION

3.1. Introduction

Three heat pipes were built and tested in the HPTF. A conventional stainless steel heat pipe was first tested to demonstrate the proper operation of the HPTF, ensure reasonable accuracy in procedures and measurements, and obtain baseline data for comparison with the fabric composite designs. Two fabric composite heat pipes, one heavy and one lightweight, were built and tested. Water was used as the working fluid in all three heat pipes. Each of these heat pipes are described in detail in this chapter. A very lightweight fabric composite reflux tube, designed and built at Battelle, is currently being tested using the HPTF. A brief description of the reflux tube is also provided.

3.2. Conventional Heat Pipe

The conventional heat pipe consists of a standard 2.54 cm (1 in) ID, 3.2 mm (125 mil) thick 304 stainless steel tubing section as the structure. This heat pipe is 81.5 cm (32 in) in length and has a threaded end piece on the condenser end to allow access for fitting of the wick. The threaded end piece is equipped with a 0.3175 cm (1/8 in.) tube which is coupled through the teflon end piece on the test chamber to facilitate the evacuation of the heat pipe and the loading of the working fluid. The heat pipe wick is a 0.5 mm (20 mil) braided Nextel (trademark of the

3M Company, Saint Paul, MN) fabric tubing which was obtained from Battelle Pacific Northwest Laboratories. Tests previously conducted at Oregon State University demonstrated satisfactory wicking characteristics for the Nextel fabric [1]. The wick was loaded in the stainless steel heat pipe by first sliding it over a 0.64 cm (1/4 in) diameter dowel and then inserting it into the full length of the heat pipe. This method allowed loading of the wick without any twisting or cramming, and the wick fit so snugly that no wire spring or screen was needed to hold it against the inside of the pipe. A post-test examination of the wick showed that the wick remained firmly attached to the wall of the heat pipe. The threaded end piece on the condenser section of the heat pipe provided a pressure tight seal and easy access to the wick.

3.3. Fabric Composite Heat Pipes

The fabric composite (FC) heat pipes are generally similar in design to the conventional heat pipe described above, but the condenser section is sleeved with an aluminoborosilicate (Nextel) fabric. Because the fabric is woven into a tube shape, it can be compressed axially to increase the diameter which makes it easy to slide over the pipe. Once on the pipe, the fabric tubing is stretched axially, shrinking the diameter and creating good contact between the stainless steel and the fabric. Ideally, the braided aluminoborosilicate tube would provide all the structural strength for the heat pipe, and the metal liner would serve only to contain the working fluid. The fabrication of such heat pipes is complicated. Such fabrication

techniques have been developed (at great expense) by Battelle Pacific Northwest Laboratory [2,3]. It is possible, however, to test the thermal performance of the fabric composite concept without getting too elaborate in the fabrication. This is precisely what was done in the design of the two fabric composite heat pipes.

The "heavyweight" fabric composite heat pipe is nothing more than the conventional stainless steel heat pipe described above, fitted with an aluminoborosilicate sleeve on the condenser section. By adding a layer of fabric to the conventional heat pipe, the effect of the fabric on the radiative properties of the heat pipe can be directly observed. An effort was made to ensure the tightest possible fit of the fabric tubing to minimize the contact resistance between the liner and the fabric. This contact resistance has been shown to have a significant effect on the heat transfer and effective emissivity of the composite radiator [3].

The fabric composite design was then taken a step further. Using a 2.54 cm OD x 0.25 mm (1 in x 10 mil) stainless steel tube for the liner, and a layer of aluminoborosilicate fiber as described above, a "lightweight" fabric composite heat pipe was constructed. The thin-wall stainless steel was welded at one end to a 3.2 mm thick stainless steel end piece (approximately 18 cm long). The thick end piece serves as the evaporator section of the fabric composite heat pipe and allows the band heaters to be attached without damaging the metal liner. The lightweight condenser section is 63 cm in length. At the condenser end, a rigid condenser cap houses the heat pipe evacuation and charging line. This end piece seals the heat pipe using a threaded sleeve insert. While this method was feasible with the 0.25

mm liner, thinner, less rigid, foil liners will require more sophisticated methods for sealing the condenser end. The end pieces are also designed to facilitate the suspension of the heat pipe in the test chamber. The general configuration of the FC heat pipe was shown previously in Figure 1.7.

Additional tests were conducted on the lightweight FC design to determine the effects of reducing the thickness of the metal liner. Theoretically, when the thickness of the liner is reduced, the temperature drop due to conduction across the metal is smaller, and the heat pipe rejects heat at higher temperatures. Since the radiated power is a function of the temperature to the fourth power, this should also improve the performance of the heat pipe radiator. The lightweight FC heat pipe, while superior to the heavyweight heat pipe described above, is still far from an optimized design. At 0.25 mm, the stainless steel liner is still thick enough to be quite rigid and provide structural strength for the heat pipe. Ideally, the liner would consist of a very thin layer (as thin as 50 to 100 μm), whose sole purpose is to contain the working fluid [4].

3.4. Lightweight Fabric Composite Reflux Tubes

The HPTF is currently being used to conduct life tests on a fabric composite reflux tube, designed and built at Battelle Pacific Northwest Laboratories. The reflux tube is of a more sophisticated fabrication than the lightweight FC heat pipe described in Section 3.3. The reflux tube uses the same Nextel fabric tubing for the condenser section and a 2 mil. copper foil as the liner. An 8 cm length of 0.25

mm thick copper tubing is used for the evaporator end to allow a heater to be attached. The thin copper foil is very fragile, and the heat pipe must be pressurized in order to have sufficient structural stability to allow loading into the HPTF. The reflux tube, unlike the heat pipe, has a wick only on the evaporator section of the tube, so the working fluid is returned to the evaporator by gravity. The reflux tube is operated in the vertical position, so the HPTF (refer to Figure 2.1) was turned and set on its closed end to conduct the life tests. The results of these tests will be presented in the M.S. Thesis of Ross Snuggerud [5].

3.5. Conclusion

One conventional heat pipe and two fabric composite heat pipes have been built for testing in the HPTF. The conventional heat pipe tests are used to verify the proper operation of the test facility, and for comparison to the FC heat pipe tests. The design of the FC heat pipes, while not optimal, is sufficient to demonstrate the improvement in the heat pipe radiator performance.

3.6. References

1. Marks, T.S., "An Investigation of Fabric Composite Heat Pipe Feasibility Issues," M.S. Thesis, Oregon State University, Corvallis, OR, 1992.

2. Pauley, K.A., Z.I. Antoniak, L.L. King, and G.H. Hollenberg, "Design and Testing of Ultralight Fabric Reflux Tubes," *Proc. 10th Symposium on Space Nuclear Power Systems*, Albuquerque, NM, Jan. 10-14, 1993.

3. Antoniak, Z.I, B.J. Webb, J.M. Bates, and M.F. Cooper, "Construction and Testing of Ceramic Fabric Heat Pipe With Water Working Fluid," *Proc. 8th Symposium on Space Nuclear Power Systems*, CONF-910116, Albuquerque, NM, 1991.

4. Antoniak, Z.I, W.J. Krotiuk, B.J. Webb, J.T. Prater, and J. M. Bates, *Fabric Space Radiators*, PNL-6458, Pacific Northwest Laboratory, Richland, WA, 1988.

5. Personal communication with R. Snuggerud, M.S. Thesis to be completed in Jan. 1993.

CHAPTER 4. RESULTS AND ANALYSIS

4.1. Introduction

The purpose of the heat pipe tests is to evaluate the radiant properties of the fabric composite and compare them with the properties of a conventional stainless steel heat pipe. These tests were first conducted on the conventional heat pipe and the emissivity of the stainless steel surface was empirically determined. Similar tests were then performed on the fabric composite heat pipes and the emissivity of the fabric condenser surface was calculated. This chapter contains an analysis of the startup and steady state operation of these heat pipes including frozen heat pipe startup and wick dryout. The final results show a significant improvement in emissivity and capacity of heat pipes using the fabric composite design.

4.2. Method of Evaluation

4.2.1. Calculation of Heat Pipe Emissivity.

The primary objective of the heat pipe tests was to calculate the effective emissivity of the fabric composite heat pipes. The equation for the radiation heat transfer between the heat pipe condenser and the vacuum chamber walls, Equation 2.1 can be solved for the emissivity of the heat pipe ε_{hp} to obtain Equation 4.1. The dimensions of the heat pipe, the temperature of the heat pipe condenser and vacuum chamber surfaces, and the heat pipe power dissipation, Q, are determined

$$\varepsilon_{hp} = \frac{Q}{\sigma A_{hp}(T_{hp}^4 - T_{vc}^4) - Q\left(\frac{1-\varepsilon_{vc}}{\varepsilon_{vc}}\right)\left(\frac{r_{hp}}{r_{vc}}\right)^2} \tag{4.1}$$

experimentally. Equation 4.1 is then used to calculate the heat pipe emissivity. The power dissipated by the heat pipe by radiation to the vacuum chamber walls is determined by measuring the power supplied to the heat pipe evaporator, determined by Equation 4.2, and correcting for the amount of heat lost from the evaporator end.

$$P = V_{htr} \cdot I_{htr} \tag{4.2}$$

The amount of heat lost at the evaporator end is determined by the radiation heat transfer between the evaporator thermal shield and the vacuum chamber wall.

$$Q_{loss} = \frac{\sigma A_{sh}(T_{sh}^4 - T_{vc}^4)}{\frac{1}{\varepsilon_{sh}} + \frac{1-\varepsilon_{vc}}{\varepsilon_{vc}}\left(\frac{r_{hp}}{r_{vc}}\right)^2} \tag{4.3}$$

Equation 4.3 is of the same form as Equation 2.1 with the inner radiant surface being the outermost evaporator shield.

Recall from Chapter 2 that heat loss by conduction is assumed to be negligible, and thus, Q_{loss} is a result of radiation heat transfer from the evaporator across the radiation shields and to the vacuum chamber walls. A FORTRAN program for evaluating the above equations was written and is provided in Appendix B.

4.2.2. Analysis of Heat Pipe Operation.

In addition to the calculation of emissivity, the behavior of each heat pipe is discussed using a plot of the heat pipe pressure, evaporator temperature, and condenser temperature during operation. Values for the saturation temperature were also determined and included in the graphs in order to verify heat pipe operation in saturated conditions and to estimate the temperature drop across the wall of the heat pipe. In all cases, the plotted saturation temperature is consistent with that expected based on the ΔT across the fabric and lining. The saturation temperature is also of interest because the band heaters did not provide a very uniform heat input to the evaporator and several difficulties are associated with the measurement of the evaporator temperature. The temperatures measured by the evaporator thermocouples is believed to be in error by as much as 10°C, since the heaters generally had better contact with the thermocouples than with the evaporator surface. Additionally, the very large temperature gradient between the heaters, the thermocouples, and the evaporator give way to significant errors in the temperature measurement. The thermocouple voltage is generated at the location of the temperature gradient, and not necessarily at the thermocouple junction [3]. The

highest temperature gradient exists where the thermocouple wires pass under the band heaters, and can be expected to be very large. In other words, the evaporator thermocouples provide a better measurement of the heater temperature than the heat pipe evaporator temperature. One additional contribution to the error in this temperature measurement might be attributed to the effect of the heater coil emf on the thermocouple. All of these factors most likely contribute to the error in the evaporator temperature measurement, and help explain the excessive ΔT between the evaporator and condenser. Fortunately, the evaporator temperature is not used in any of the calculations.

The tests performed on each of the three heat pipes are presented in the following sections. Both startup and steady state operation are plotted and evaluated.

4.3. Conventional Heat Pipe

The startup of the conventional heat pipe was commenced from the frozen state. This differs from the majority of tests conducted in that the working fluid was loaded prior to warming up the heat pipe. It was found that if the facility was cold, excessive moisture would accumulate in the vacuum chamber, so that the heat pipe was loaded into the HPTF, and the chamber was evacuated, prior to cooling. The presence of moisture in the vacuum chamber had an adverse effect on the thermocouples and instrument wiring. The normal procedure was to load the working fluid once the entire length of the condenser section had been heated to above 0°C. However, during this test, the heat pipe had a sufficient amount of

working fluid remaining in the wick from a previous test. Additionally, enough moisture was in the evacuation line to block it upon freezing, and the heat pipe pressure was not observable until well into the startup when the evacuation line had thawed. The frozen startup is discussed more fully in Section 4.8.

Figure 4.1 shows the behavior of the conventional stainless steel heat pipe during startup. Once the heat pipe was loaded into the HPTF, a vacuum was drawn on the test chamber and heat pipe. Power was then supplied to the evaporator end by the band heaters, and the voltage and current to the heaters was measured. An initial power of 39 W, which had produced steady state operation in previous heat pipe tests, was used to startup the heat pipe. During startup, the evaporator and condenser temperatures increase steadily, and the temperature along the length of the

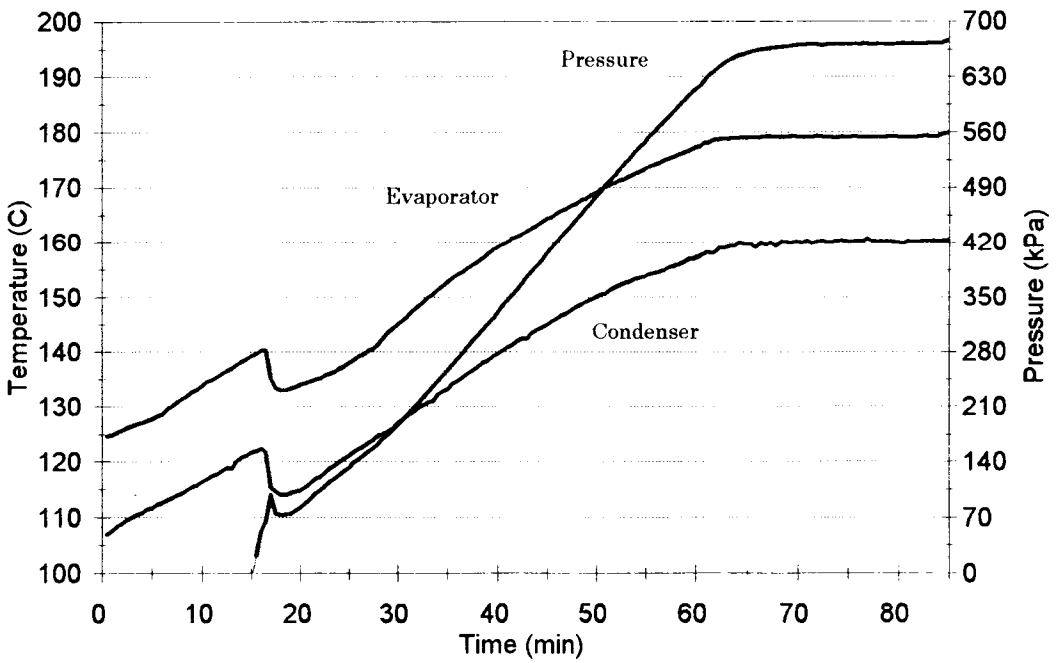

Figure 4.1. Conventional Heat Pipe, Startup

condenser is relatively isothermal. Once saturation is achieved, the pressure begins to rise rapidly. Both the temperature and the pressure increase linearly until an equilibrium temperature and pressure is reached for the heat pipe operation. At this temperature, the heat pipe radiates energy at a rate equal to the energy addition at the evaporator.

After 70 minutes, the heat pipe reached a steady state condition with the condenser temperature at approximately 160 °C. Then in an effort to increase the steady state temperature, the power was then increased to 47 W (50 V). Figure 4.2 shows the steady state operation. The temperature and pressure rise linearly again

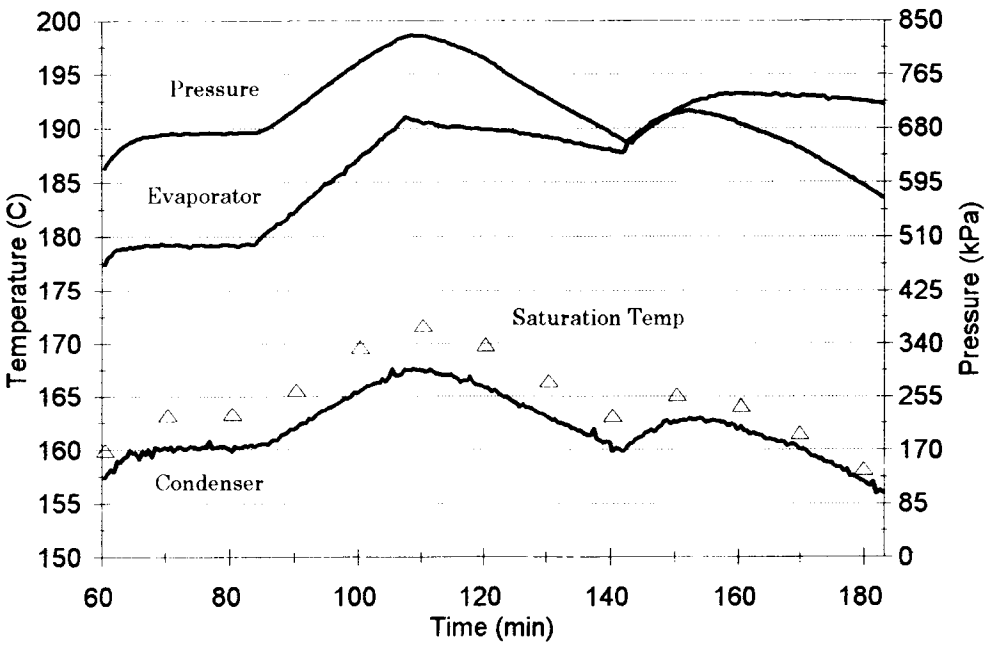

Figure 4.2. Conventional Heat Pipe, Steady State

due to the increase in the power input. As the evaporator temperature approached 200°C, the power was returned to 39 W (45 V) to prevent drying out the wick and to maintain steady state operation for calculations. The heat pipe was secured and the test concluded after 183 minutes of operation.

The heat pipe was evaluated at a power input of 39 W with the condenser temperature at 166°C. The heat loss was calculated to be 3.9 W, and the resulting heat pipe emissivity ε_{hp} was 0.32. Error analysis was performed and is discussed in Section 4.8.

4.4. Heavyweight Fabric Composite Heat Pipe

Startup of the heavyweight fabric composite heat pipe, shown in Figure 4.3, was performed at a slower rate than for the conventional heat pipe in Figure 4.1.

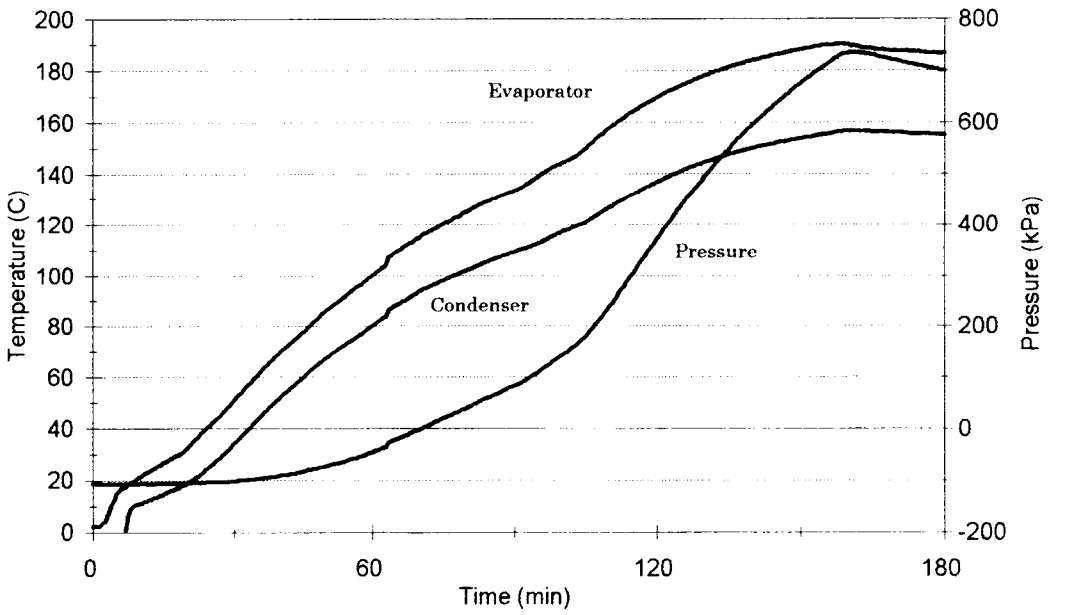

Figure 4.3. Heavyweight Fabric Composite Heat Pipe, Startup

The power applied during the initial heat up phase was 48 W (50 V). The power level was increased to 58 W (55 V) 90 minutes into the startup, and to 69 W (60 V) after 100 minutes. The improvement in the capacity of the fabric composite heat pipe was immediately apparent, as it could handle nearly twice the heat input observed during the previous conventional heat pipe test. The heat pipe reached steady state after approximately 165 minutes.

Figure 4.4 shows the steady state operation of the heavyweight fabric composite heat pipe. At 150 minutes, the power was reduced to 62 W (57 V) to limit the evaporator temperature to less than 200°C. This power level produced a slowly decreasing temperature profile, and when the evaporator temperature

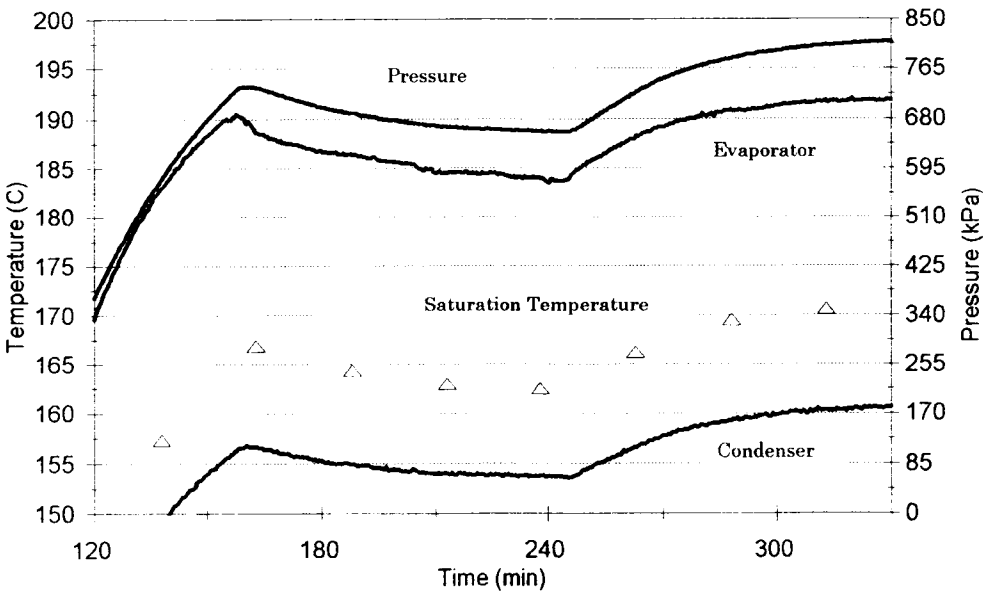

Figure 4.4. Heavyweight Fabric Composite Heat Pipe, Steady State

continued to decrease below 185°C 240 minutes into the test, the power was increased to 69 W (60 V) again. The heat pipe was operated at a power of 69 W until the test was secured after 336 minutes. An input of 69 W was observed to produce a relatively steady operation in the fabric composite heat pipes.

The heavyweight fabric composite heat pipe was evaluated at 68.4 W, with a condenser temperature equal to 157°C. The estimated heat loss at the evaporator end was 6.7 W, and the emissivity ε_{hp} was calculated to be 0.62. Error analysis is contained in Section 4.8

4.5. Lightweight Fabric Composite Heat Pipe

Based on the experience from the previous fabric composite heat pipe test, a smooth startup and long steady operation of the lightweight FC heat pipe was achieved. The lightweight heat pipe was started up using a gradually increasing power from 18 to 69 W so as to approach the steady operating temperature and power level at a slower rate, and prevent the overshoot seen in the previous test. Figure 4.5 provides a plot of the heat pipe pressure and the evaporator and condenser temperatures during the smooth approach to power. Once a steady state condition was achieved with the input power at 69 W, the lightweight fabric composite heat pipe was evaluated for nearly four hours. Figure 4.6 shows the long, steady run at 69 W power input.

A refinement in the testing procedure is evident from the results of the steady operation of the lightweight heat pipe. During the almost four hours of steady state

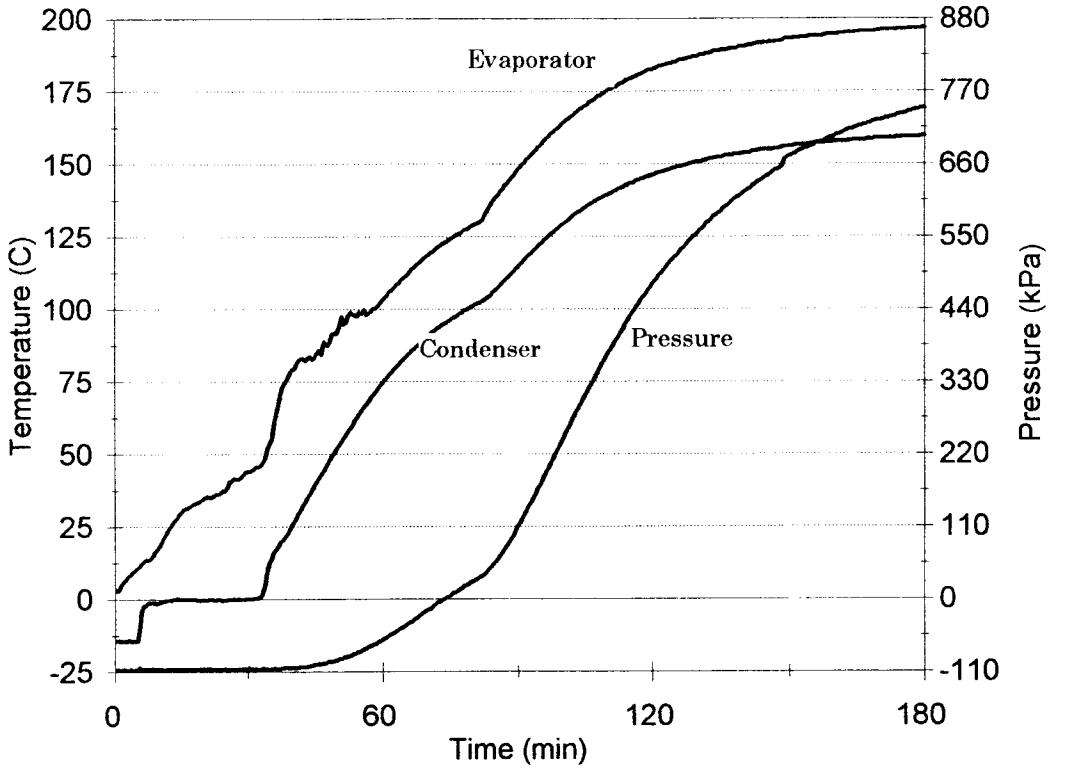

Figure 4.5. Lightweight Fabric Composite Heat Pipe, Startup

operation, the condenser temperature remained within ± 3°C of the temperature used to evaluate the heat pipe emissivity. The noise associated with the evaporator temperature measurement, as discussed in Section 4.1.2, is apparent in Figure 4.6.

The lightweight fabric composite heat pipe was evaluated at 69 W and 159°C. Evaporator heat loss was estimated to be 6.1 W, and the heat pipe emissivity ε_{hp} was 0.69. The uncertainty in the experimental results is treated in Section 4.8.

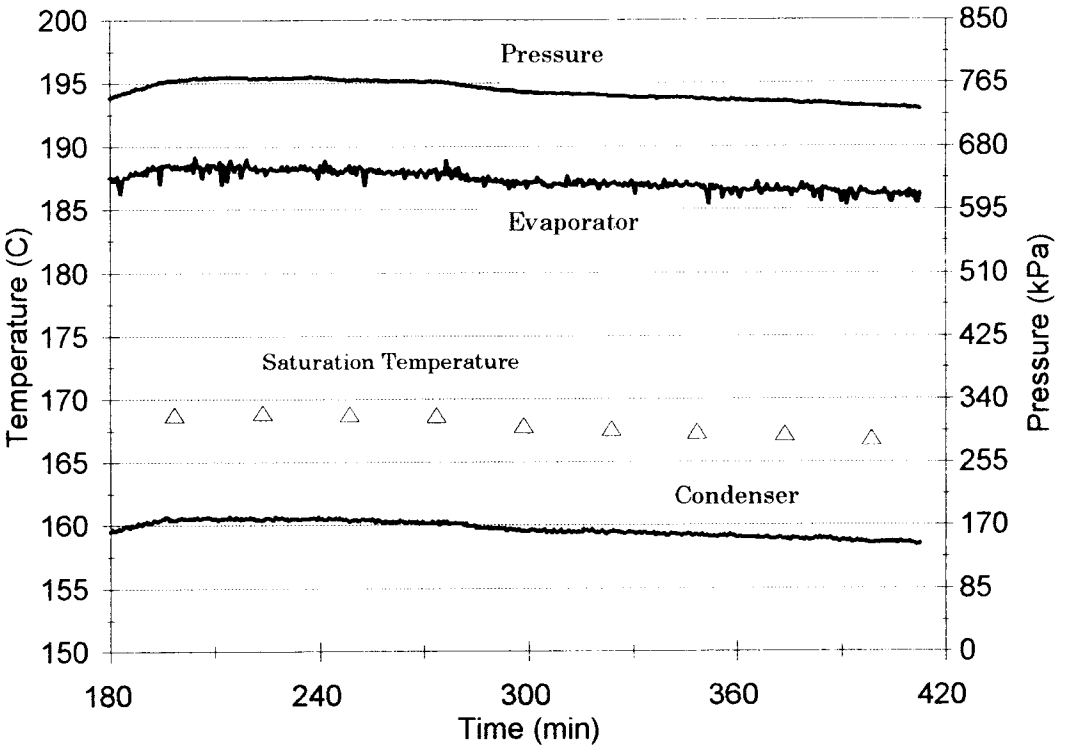

Figure 4.6. Lightweight fabric Composite Heat Pipe, Steady State

4.6. Frozen Heat Pipe Startup

Heat pipe startup from a frozen state was mentioned in Section 4.3. A plot of the heat pipe parameters during this startup is provided in Figure 4.7. Two aspects of the startup are apparent from the graph. During startup of all of the heat pipes, the temperature of the condenser was seen to increase slowly, but with less of a time lag than seen for the frozen case. In the frozen heat pipe experiment, the temperature along the length of the condenser rises as the pipe is heated, but it took an appreciable amount of time to thaw out the end of the condenser. During an

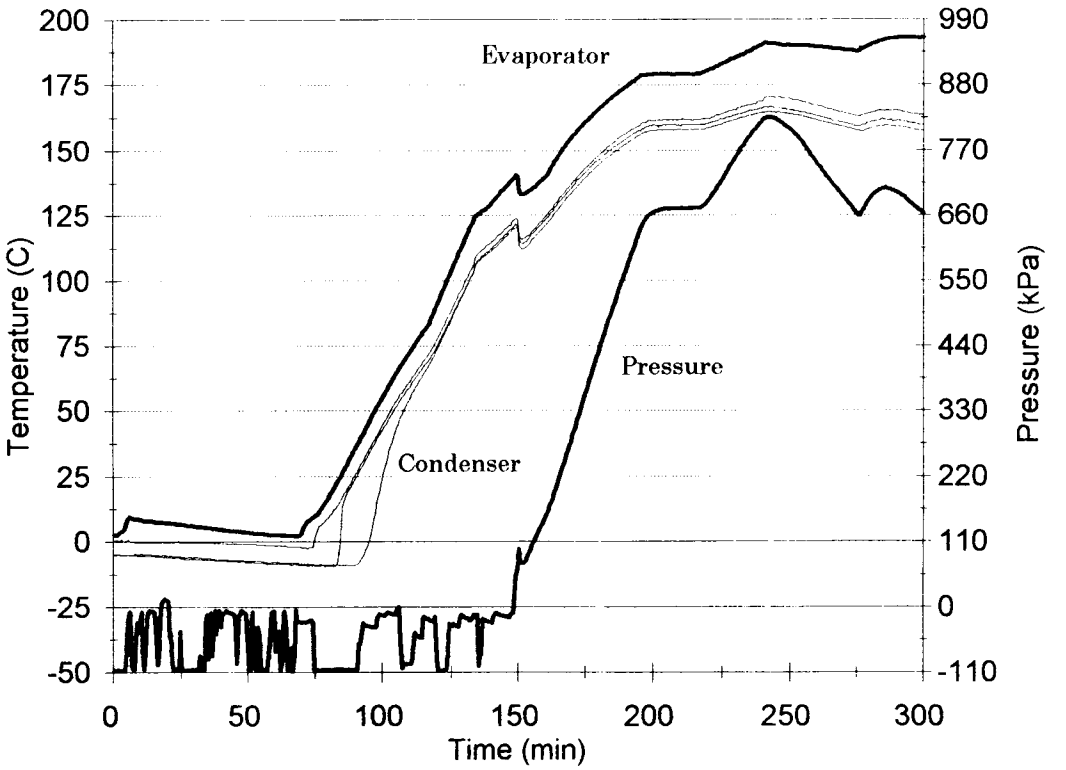

Figure 4.7. Frozen Heat Pipe Startup.

unfrozen startup, the axial condenser temperature is nearly isothermal due to the formation and flow of vapor in the pipe. The condenser temperature is plotted for several locations along the length of the pipe to show how the isothermal condition is reached only after the water in the wick has thawed. Once the entire length of the condenser had been thawed, at about 150 minutes, the startup proceeded normally, and the condenser temperature increased rapidly.

Note that the heat pipe pressure measurement was not available until after the condenser was completely thawed. This is due to blockage of the heat pipe

evacuation and fill line where the pressure transducer is connected. A sudden dip in the pressure and temperature occurred when the evacuation line became clear, allowing the vapor in the heat pipe to expand and fill the evacuation line.

4.7. Wick Dryout

During an approach to steady state power for one of the fabric composite heat pipe tests, a "dryout" condition occurred. Dryout occurs when the capillary pumping limit of the wick is exceeded and the working fluid is evaporated faster than it can be replenished. Once dryout occurs, the heat pipe will not operate until the wick has been rewetted or "quenched." Figure 4.8 shows the effects of dryout on the heat pipe

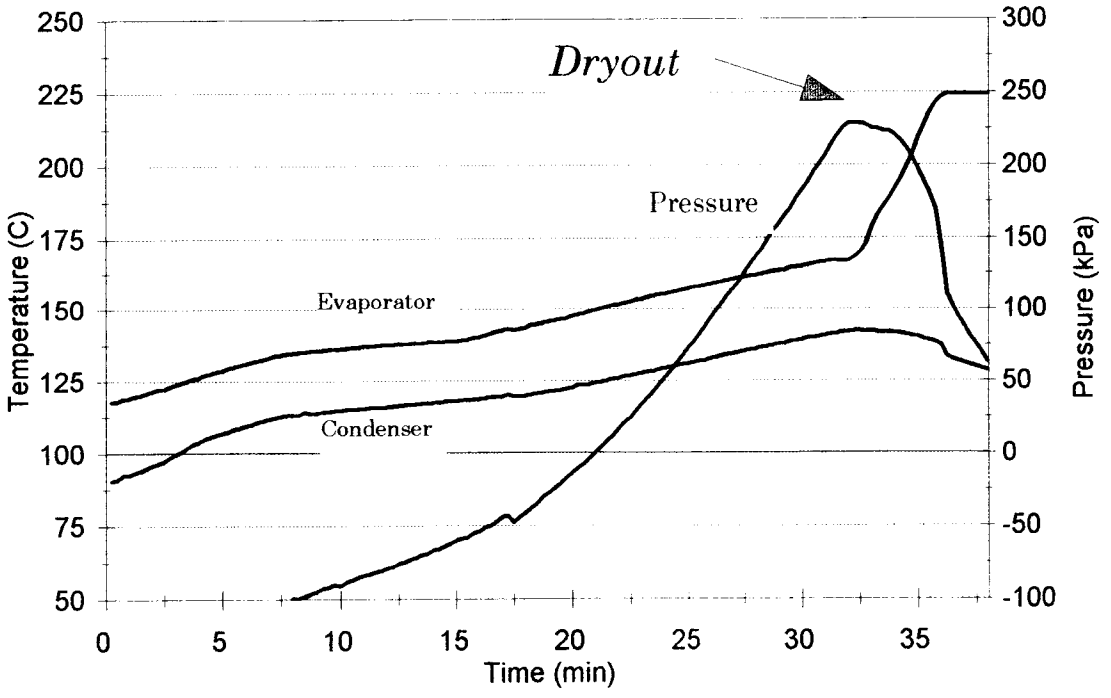

Figure 4.8. Wick Dryout During Heat Pipe Startup

operation. When dryout is achieved, the heat pipe pressure drops rapidly, and the absence of continued evaporation, results in a loss of cooling, causing the evaporator temperature to increase dramatically. The condenser temperature decreases, following the saturation temperature.

It was found that once dryout had occurred, the heaters had to be shut off and the heat pipe completely cooled down in order to rewet the wick and begin another test. While the dryout condition was not intended during the test, it did provide data to experimentally evaluate the fabric composite heat pipe limits. A complete analysis of the dryout phenomenon for the heat pipe is not provided here, but is left for future work.

4.8. Error Analysis

When making calculations in radiation heat transfer, a large degree of uncertainty is attributable to the value used for the emissivity of the radiating surfaces. The emissivity of a material is dependent upon the properties of the material as well as the conditions under which it is radiating. For example, the emissivity of stainless steel is found to be from 0.16 to 0.39 depending on the type of alloy, surface treatment, and the temperature of the surface. The effect of the surface condition is particularly difficult to specify with confidence. The surfaces of concern in the heat pipe tests are the vacuum chamber wall, and the evaporator shield. The emissivity of these surfaces must be estimated and used in the

calculation of the heat pipe emissivity, and the uncertainty in these estimates contributes to the overall uncertainty in the calculated value for ε_{hp}.

The interior wall of the vacuum chamber is relatively smooth and painted with a flat black lacquer. The emissivity of the vacuum chamber wall, ε_{vc}, can therefore be estimated to be from 0.96 to 0.98. The value of ε_{vc} estimated for use in the calculations was 0.94 ± 0.04. The value is reduced somewhat to account for scratches and bare spots on the vacuum chamber wall, and the uncertainty of $\pm$ 0.04 covers the range of reasonable values of ε_{vc}.

The emissivity of the stainless steel shields (ε_{sh}) is more difficult to estimate. The surface is not polished, but it is relatively smooth and free of oxidation. The expected range of ε_{sh} is from 0.2 to 0.4, so a value of 0.3 ± 0.1 was used.

Uncertainties also exist in the measured parameters. These uncertainties arise due to the accuracy and tolerance of the instrumentation, which was discussed in Chapter 2. The uncertainties δx_i , or fractional uncertainties $\delta x_i/x_i$, for the values measured in the heat pipe tests are listed in Table 4.1. The uncertainties were derived from the instrument specifications, data acquisition system accuracy, and observed characteristics of the data such as noise, fluctuations, and contact resistance. The uncertainties were assumed to be random and independent. Combined and total uncertainties were calculated using the sum in quadrature method [5]. A routine to calculate the uncertainties associated with each experiment is included in the data evaluation program listed in Appendix B. The resulting uncertainties for the emissivities calculated above are shown in Table 4.2.

Table 4.1. Uncertainty in Measured Values.

MEASURED PARAMETER	UNCERTAINTY δx_i or $(\delta x_i/x_i)$
V	± 0.5 V
I	± 0.1 A
Q_{in}	± 0.059
A	≈ 0
T_{vc}	± 2 °C
T_{hp}	± 2 °C
ε_{vc}	± 0.04
ε_{sh}	± 0.1
P	± 10 kPa

Table 4.2. Overall Uncertainty in Calculated Values.

HEAT PIPE	δQ (W)	$\delta\varepsilon_{hp}$
Conventional	± 2	± 0.02
Heavyweight FC	± 3	± 0.04
Lightweight FC	± 3	± 0.04

The final uncertainty in the calculated heat pipe emissivity is approximately 6% for each of the tests discussed. This is a reasonable level of uncertainty for experimental results, and supports the credibility of the procedures for testing and evaluating the performance of the heat pipes in the HPTF.

4.9. Summary and Conclusion

The results of the emissivity calculations are summarized in Table 4.3. The tests demonstrated a significant enhancement in the radiant heat transfer due to the properties of the fabric composite. These results correlate well with those reported by Antoniak and Webb in 1991 [6], and more recent studies of fabric emissivities conducted at Oregon State University [7].

Table 4.3. Summary of Experimental Results

HEAT PIPE	POWER (W)	T_{Cond} (°C)	EMISSIVITY
Conventional	39 ± 2	166 ± 2	0.32 ± 0.02
Heavyweight FC	68 ± 3	158 ± 2	0.62 ± 0.04
Lightweight FC	69 ± 3	160 ± 2	0.68 ± 0.04

The results are significant because of the multiple improvements to radiator efficiency inherent in the fabric composite design. The increased emissivity is an important advantage of the fabric composite, but this could also have been achieved by notching the steel heat pipe, or by simply painting it black. However, the combined advantages of *higher* output capacity and *lower* mass associated with the fabric composite, and the possibility of improved survivability, should make the use of fabric composite heat pipe radiators an attractive choice in the design of future space power systems. An appreciation for the magnitude of the savings possible in system mass can be gained from Table 4.4. The overall advantage of the fabric

composite design is best shown by the power to mass ratio for each heat pipe. In the simple design tested in the HPTF, for example, the heat rejection capacity nearly doubled, while the heat pipe mass was reduced by a factor of three.

Table 4.4. Summary and Comparison of Heat Pipe Designs

HEAT PIPE DESIGN	LINER THICKNESS	COMPOSITE	MASS (g)	POWER/MASS (W/kg)
Conventional	3.2 mm	-----	1530	25
Heavyweight FC	3.2 mm	Stainless/Nextel	1530	45
Lightweight FC	0.25 mm	Stainless/Nextel	510	135
FC Reflux Tube	50 μm	Copper/Nextel	140	500

The tests conducted on the fabric composite heat pipes using the HPTF not only verify the feasibility of such heat pipes as potential space radiators, but show that such a design has significant advantages over many conventional design concepts.

4.10. References

1. Siegel, R., and J.R. Howell, *Thermal Radiation Heat Transfer*, 2nd Ed., Hemisphere, New York, 1981.

2. Incropera, F.P., and D.P. Dewitt, *Fundamentals of Heat and Mass Transfer*, 2nd Ed., John Wiley & Sons, New York, 1985.

3. *Temperature Measurement Handbook and Encyclopedia*, Omega Engineering Inc. Stamford, CT, 1984.

4. Moffat, R.J., "Describing Uncertainties in Experimental Results," *Experimental Thermal and Fluid Science*, **1**, 1988, pp. 3-17.

5. Taylor, J.R., *An Introduction to Error Analysis: The Study of Uncertainties in Physical Measurements*, University Science Books, Mill Valley, CA, 1982.

6. Antoniak, Z.I, B.J. Webb, J.M. Bates, and M.F. Cooper, "Construction and Testing of Ceramic Fabric Heat Pipe With Water Working Fluid," *Proc. 8th Symposium on Space Nuclear Power Systems*, CONF-910116, Albuquerque, NM, 1991.

7. Klein, A.C., Z. Gulsha-Ara, W.C. Kiestler, R.D. Snuggerud, and T.S. Marks, "Fabric Composite Heat Pipe Technology Development," *10th Symposium on Space Nuclear Power Systems*, Albuquerque, NM, Jan. 10-14, 1993.

CHAPTER 5. CONCLUSIONS AND RECOMMENDATIONS

5.1. Significance of Test Results

Heat pipes have played a significant role in the development of space based thermal management systems. Their simplicity, reliability, and unique capability for heat transfer make them ideal for use in space power systems. Many of the space nuclear power systems currently being designed rely upon heat pipe radiators for waste heat rejection. Advanced designs that improve the efficiency of these heat pipe radiators could have a significant effect on the overall system feasibility. A fundamental design consideration for any space based system is the total system mass. Thus, a design solution with the potential for reducing the mass of the radiator assembly without sacrificing its capacity for heat rejection is of profound interest. The results of the tests conducted on the fabric composite heat pipes show that fabric composite radiators could be used to improve radiator efficiency while significantly reducing the system mass.

The primary objective of the tests conducted in the HPTF was to demonstrate the ability to enhance radiative heat rejection through the use of a fabric composite. Using the fabric composite design, the emissivity of a stainless steel heat pipe was increased from 0.32 to 0.62, and a more advanced, lightweight fabric composite design achieved an emissivity of 0.69. The increased emissivity, combined with the reduction in heat pipe mass, resulted in a greater than 500% improvement in the radiator power to mass ratio. These results are summarized in Table 5.1.

Table 5.1. Summary of Experimental Results

HEAT PIPE	Conventional	Heavyweight FC	Lightweight FC
T_{cond}	166°C	158°C	159°C
T_{evap}	188°C	191°C	188°C
T_{SAT}	170°C	171°C	167°C
Pressure	800 kPa	805 kPa	744 kPa
Q_{in}	39 W	68 W	69 W
Q_{loss}	4 W	6 W	6 W
ε	0.32 ± 0.02	0.62 ± 0.04	0.69 ± 0.04
Mass	1530 g	1530 g	510 g
Power/Mass (W/kg)	25	45	135

Clearly, the fabric composite design concept offers a promising and feasible method for improving space radiator performance. Fabric composite heat pipes could be used in future space power systems to reduce the overall mass of the system and improve system efficiency, reliability, and survivability.

5.2. Recommendations for Future Work

Both of the heat fabric composite heat pipes tested during this work were relatively rigid and heavy. The next logical step in the use of the HPTF is to test a very lightweight heat pipe similar in design to the Battelle fabric composite reflux tube described in Chapter 3. The HPTF is currently being used to test the reflux tube in the vertical position, but could be returned to the horizontal position to test

a lightweight fabric composite heat pipe. The heat pipe mounting rack is designed to accommodate these lightweight heat pipes by supporting them at the ends. The fabrication of these heat pipes is more complex and costly, but if such work is supported in the future, it is recommended that an ultralight fabric composite heat pipe be built and tested in the HPTF.

The HPTF was also designed to enable the testing of multiple heat pipes. It would be a relatively simple procedure to modify the heat pipe mounting rack to support a bank of two or three heat pipes which could then be tested in the HPTF.

Finally, tests of heat pipes using alternative fabrics could be done in the same manner that the aluminoborosilicate (Nextel) fabric was tested. The properties of various fabrics and composites (eg. copper/Nextel, copper/silicon carbide, stainless/astroquartz) could be evaluated in the HPTF.

APPENDICES

APPENDIX A. Data Acquisition Program

```
10 '-------------------------------------------------------------------------------
12 '   This Program reads 16 K-type thermocouples using the DAS-8 Board
13 ' and one EXP-16 Multiplexer, and one pressure transducer using a
14 ' second EXP-16 (Channel 0). The thermocouples are provided with cold
15 ' junction compensation in the EXP-16. The pressure Transducer has been
16 ' Calibrated such that zero volts corresponds to atmospheric pressure.
17 ' Vacuum pressure (-101 kPa) corresponds to approximately -17.0 mv with
18 ' about +/- 0.3 mv temperature dependence.
19 '    The code (QBHP.BAS) accomplishes the following:
20 '      - Initializes the DAS-8 and loads thermocouple look up table
21 '      - Measures temperature for CJC
22 '      - Measures output voltages of thermocouples on #1 EXP-16
23 '      - Converts, corrects, and linearizes thermocouple output to
24 '        temperature in degrees C.
25 '      - Measures output voltage of pressure transducer on #2 EXP-16
26 '      - Converts and corrects to measure pressure in kPa
27 '      - Calculates the heat transfered in the test facility
28 '        (calorimetric)
29 '      - Estimates heat pipe emissivity based on calorimetric
30 '      - Displays output
31 '      - Writes output to data file
40 '-------------------------------------------------------------------------------

' ********** Initialize an integer array D%(15) to receive data **********

   DIM D%(16)  '16 elements, one for each EXP-16 channel

' ***  Also initialize a corresponding real array to receive temperature data **
   DIM T(16)
   DIM LT%(16)
   DIM Sum(16)
   COMMON SHARED D%(), LT%()
   DECLARE SUB das8 (mode%, BYVAL dummy%, FLAG%)

55 OPEN "HPR.DAT" FOR OUTPUT AS #2
56 DT$ = DATE$
57 TM$ = TIME$
60 PRINT #2, "HEAT PIPE TEST ", DT$, "  Start Time = ", TM$
   PRINT #2, ""
```

```
    PRINT #2, "Time  Press  T0    T1    T2    T3    T4    T5    T6    T7    T8
T9    T10   T11   T12   T13   T14   delta T "
    PRINT #2, "-------------------------------------------------------------------------------"
    PRINT #2, ""
    CLOSE #2
70  CLS
150 SCREEN 0, 0, 0: KEY OFF: CLS : WIDTH 80
160 '
300 'For use with this code, the first EXP-16 output channel should be
305 'connected to DAS-8 channel #0 and the CJC channel to DAS-8 channel #7.
320 'The second EXP-16 is connected to DAS-8 Channel 1 (Jumpers on EXP-16).
325 '
330 ' ***************** Initialize DAS-8 ********************
370 '
380 CLEAR , 49152!
440 OPEN "DAS8.ADR" FOR INPUT AS #1
450 INPUT #1, BASADR%   'initialize & declare CALL parameters
460 CLOSE #1
480 FLAG% = 0
490 MD% = 0             'Mode 0 = initialization
500 CALL das8(MD%, VARPTR(BASADR%), FLAG%)
510 IF FLAG% < > 0 THEN PRINT "INSTALLATION ERROR"
520 '
530 '********* Load thermocouple linearizing look up data **********
540 GOSUB 50000
542 '************** Get gain setting of EXP-16's ********************
545 AV0 = 606   ' Gain setting on #1EXP-16
547 AV1 = 50    ' Gain setting on #2EXP-16
550 '
575 INPUT "Enter initial pressure transducer voltage (mv) ", IP
    INPUT "Enter mass flow rate (gpm) ", Mf
    INPUT "Enter delta T correction (C) ", corr
    CLS
    PC = (101.5 / IP) * 1000   ' initializes pressure reading
    '
595 TIN = TIMER
600 J = 0
    FOR N = 0 TO 15
    Sum(N) = 0
    NEXT N
    SUMP = 0
602 FOR J = 1 TO 66
605 '************* Get cold junction compensation temperature *************
610 'Output of CJC channel is scaled at 24.4mV/deg.C. This corresponds to
```

```
620 '0.1 deg.C./bit. Dividing output in bits by 10 yields degrees C.
630 '
640 'Lock DAS-8 to channel #7 (CJC channel selected) using mode 1
650 MD% = 1: LT%(0) = 7: LT%(1) = 7
660 CALL das8(MD%, VARPTR(LT%(0)), FLAG%)
670 IF FLAG% <> 0 THEN PRINT "ERROR IN SETTING CJC CHANNEL":
END
680 'Next get CJC data from this channel using Mode 4
690 MD% = 4: CJ% = 0
700 CALL das8(MD%, VARPTR(CJ%), FLAG%)
710 'Change output in bits to real temperature
720 CJC = CJ% / 10
730 '
740 '************* Get the thermocouple data ***************************
750 CH% = 0
760 GOSUB 1000
770 ' Entry parameters are:
790 '  CH% - specifies DAS-8 channel that EXP-16 is connected to (0-7).
800 '  D%(15) - integer data array to receive data from channels.
810 '
820 '************* Convert data to volts and linearize ****************
830 'AV0 = Gain setting on Dipswitch of EXP-16 #1
840 FOR I = 0 TO 15
850 V = (D%(I))
855 V = V * 5 / (AV0 * 2048)
860 GOSUB 51000  'perform look-up linearization
870 T(I) = TC       '= TF for degrees Fahrenheit
880 NEXT I
890 '
900 '************* Display temperature data ****************************
910 LOCATE 1, 1
920 FOR I = 0 TO 14
930 PRINT USING "Channel ## temperature = #####.#  deg. C."; I; T(I)
940 NEXT I
942 PRINT
944 PRINT USING "Cold junction temperature (CJC) = ###.# deg. C."; CJC
945 '************* Steps to get pressure data *************************
946 LT%(0) = 1: LT%(1) = 1: MD% = 1
947 CALL das8(MD%, VARPTR(LT%(0)), FLAG%)
948 IF FLAG% <> 0 THEN PRINT "ERROR IN EXP CHANNEL 1": END
950 NUX% = 0
952 MD% = 14
954 CALL das8(MD%, VARPTR(NUX%), FLAG%)
```

```
955 IF FLAG% < > 0 THEN PRINT "ERROR IN EXP-16 CHANNEL
NUMBER": END
956 MD% = 4  'do 1 A/D conversion
957 CALL das8(MD%, VARPTR(D%(0)), FLAG%)
958 IF FLAG% < > 0 THEN PRINT "ERROR IN PERFORMING A/D
CONVERSION"
960 P = D%(0)
961 P = P * 5 / (AV1 * 2048)
962 P = P * PC
965 '***************** Display Pressure data ************************
966 PRINT
967 PRINT USING "HEAT PIPE PRESSURE = ####.# kPa"; P
    FOR K = 0 TO 15
    Sum(K) = Sum(K) + T(K)
    NEXT K
    SUMP = SUMP + P
    NEXT J
    FOR M = 0 TO 15
    T(M) = Sum(M) / (J - 1)
    NEXT M
    P = SUMP / (J - 1)
    DEL = T(14) - T(13)
    PRINT USING "Delta T = ##.## C"; DEL
    PRINT
     Cp = 2.294  ' kJ/kg-K
     Q = Mf * Cp * (DEL - corr) * 71.2917
    PRINT USING " HEAT TRANSFERED = ###.## W "; Q
    A = .05107 ' Area of Heat Pipe in m^2
    SIG = 5.729E-08 ' W/m^2-K
    TC = T(11)
    TH = T(5)
    TC = TC + 273.15
    TH = TH + 273.15

    EPS = Q / (A * SIG * (TH ^4 - TC ^4))
    PRINT USING " EMISSIVITY = .### "; EPS

968 '************** Write data to output file ************************
    CLOSE #2
    '$DYNAMIC
    OPEN "HPR.DAT" FOR APPEND AS #2
  tmt$ = "####.# ####.# ###.## ###.## ###.## ###.## ###.## ###.## ###.##
###.## ###.## ###.## ###.## ###.## ###.## ###.## ###.## ###.###"
    x = TIMER
```

```
970 TM = x - TIN
    TM = TM / 60!
975 PRINT #2, USING tmt$; TM; P; T(0); T(1); T(2); T(3); T(4); T(5); T(6);
T(7); T(8); T(9); T(10); T(11); T(12); T(13); T(14), DEL
995 GOTO 600 'repeat scan of channels
999 '
1000 '---- Subroutine to convert EXP-16 channels to number of bits --------
1010 'First lock DAS-8 on the one channel that EXP-16 is connected to.
1020 LT%(0) = CH%: LT%(1) = CH%: MD% = 1
1030 CALL das8(MD%, VARPTR(LT%(0)), FLAG%)
1040 IF FLAG% < > 0 THEN PRINT "ERROR IN SETTING CHANNEL":
END
1050 'Next select each EXP-16 channel in turn and convert it.
1060 'Digital outputs OP1-4 drive the EXP-16 sub-multiplexer address, so use
1070 'mode 14 to set up the sub-multiplexer channel.
1080 FOR MUX% = 0 TO 15   'note use of integer index MUX%
1090 MD% = 14
1100 CALL das8(MD%, VARPTR(MUX%), FLAG%)        'address set
1110 IF FLAG% < > 0 THEN PRINT "ERROR IN EXP-16 CHANNEL
NUMBER": END
1120 'Now that channel is selected, perform A/D conversion using mode 4.
1130 'Transfer data to corresponding array element D%(MUX%)
1140 MD% = 4  'do 1 A/D conversion
1150 CALL das8(MD%, VARPTR(D%(MUX%)), FLAG%)
1160 IF FLAG% < > 0 THEN PRINT "ERROR IN PERFORMING A/D
CONVERSION"
1170 'Now repeat sequence for all other EXP-16 channels
1180 NEXT MUX%
1190 'All done - return from subroutine
1200 RETURN
1210 '
50000 '-------- Table lookup data for K type thermocouple ----------------
50010 'Run this subroutine only in the initialization section of your program
50020 'Number of points, voltage step interval (mV), starting voltage (mV)
50030 DATA  309 ,  .2 , -6.6
50040 READ NK, SIK, SVK
50050 'Temperature at -6.6mv, -6.4mV, -6.2mV etc.
50060 DATA -353.5,-249.3,-224.0,-207.6,-194.3,-182.8,-172.3,-162.8,-153.8,-145.4
50070 DATA -137.3,-129.6,-122.3,-115.2,-108.3,-101.6, -95.1, -88.7, -82.5, -76.4
50080 DATA  -70.4, -64.6, -58.8, -53.1, -47.5, -42.0, -36.6, -31.2, -25.9, -20.6
50090 DATA  -15.4, -10.2,  -5.1,  -0.0,   5.0,  10.1,  15.1,  20.0,  25.0,  29.9
50100 DATA   34.8,  39.7,  44.6,  49.5,  54.3,  59.1,  64.0,  68.8,  73.6,  78.4
50110 DATA   83.2,  88.0,  92.9,  97.7, 102.5, 107.4, 112.2, 117.1, 122.0, 126.9
50120 DATA  131.8, 136.7, 141.7, 146.6, 151.6, 156.5, 161.5, 166.5, 171.5, 176.5
```

```
50130 DATA  181.6, 186.6, 191.6, 196.6, 201.6, 206.6, 211.6, 216.6, 221.5, 226.5
50140 DATA  231.5, 236.4, 241.4, 246.3, 251.2, 256.1, 261.0, 265.9, 270.8, 275.6
50150 DATA  280.5, 285.3, 290.2, 295.0, 299.8, 304.6, 309.4, 314.3, 319.1, 323.9
50160 DATA  328.7, 333.4, 338.2, 343.0, 347.8, 352.6, 357.3, 362.1, 366.9, 371.6
50170 DATA  376.4, 381.1, 385.9, 390.6, 395.4, 400.1, 404.8, 409.6, 414.3, 419.0
50180 DATA  423.8, 428.5, 433.2, 437.9, 442.6, 447.3, 452.0, 456.8, 461.5, 466.2
50190 DATA  470.9, 475.6, 480.3, 485.0, 489.7, 494.4, 499.1, 503.8, 508.5, 513.1
50200 DATA  517.8, 522.5, 527.2, 531.9, 536.6, 541.3, 546.0, 550.7, 555.4, 560.0
50210 DATA  564.7, 569.4, 574.1, 578.8, 583.5, 588.2, 592.9, 597.6, 602.3, 607.0
50220 DATA  611.7, 616.4, 621.2, 625.9, 630.6, 635.3, 640.0, 644.8, 649.5, 654.2
50230 DATA  658.9, 663.7, 668.4, 673.2, 677.9, 682.7, 687.4, 692.2, 696.9, 701.7
50240 DATA  706.5, 711.3, 716.1, 720.8, 725.6, 730.4, 735.2, 740.0, 744.8, 749.7
50250 DATA  754.5, 759.3, 764.1, 769.0, 773.8, 778.7, 783.5, 788.4, 793.3, 798.1
50260 DATA  803.0, 807.9, 812.8, 817.7, 822.6, 827.5, 832.4, 837.3, 842.2, 847.2
50270 DATA  852.1, 857.1, 862.0, 867.0, 872.0, 876.9, 881.9, 886.9, 891.9, 896.9
50280 DATA  901.9, 906.9, 911.9, 916.9, 922.0, 927.0, 932.0, 937.1, 942.2, 947.2
50290 DATA  952.3, 957.4, 962.5, 967.6, 972.7, 977.8, 982.9, 988.0, 993.1, 998.2
50300 DATA
1003.4,1008.5,1013.7,1018.8,1024.0,1029.2,1034.4,1039.6,1044.8,1050.0
50310 DATA
1055.2,1060.4,1065.6,1070.8,1076.1,1081.3,1086.6,1091.9,1097.2,1102.4
50320 DATA
1107.7,1113.0,1118.3,1123.7,1129.0,1134.3,1139.7,1145.0,1150.4,1155.8
50330 DATA
1161.2,1166.6,1172.0,1177.4,1182.9,1188.3,1193.8,1199.2,1204.7,1210.2
50340 DATA
1215.7,1221.2,1226.8,1232.3,1237.9,1243.5,1249.1,1254.7,1260.3,1265.9
50350 DATA
1271.6,1277.3,1282.9,1288.6,1294.3,1300.1,1305.8,1311.5,1317.3,1323.1
50360 DATA 1328.9,1334.7,1340.5,1346.4,1352.2,1358.1,1363.9,1369.8,1375.7
50370 DIM TK(NK - 1)
50380 FOR I = 0 TO NK - 1: READ TK(I): NEXT I
50390 RETURN
50400 '
51000 '****** Interpolation routine to find K thermocouple temperature *****
51010 'Entry variables:-
51020 '    CJC = cold junction compensator temperature in deg. C.
51030 '      V = thermocouple voltage in volts
51040 'Exit variables:-
51050 '     TC = temperature in degrees Centigrade
51060 '     TF = temperature in degrees Fahrenheit
51070 'Execution time on std. IBM P.C. = 46 milliseconds
51080 'Perform CJC compensation for K type
51090 VK = 1000 * V + 1! + (CJC - 25) * .0405'VK in mV
```

```
51100 '
51110 'Find look up element
51120 EK = INT((VK - SVK) / SIK)
51130 IF EK < 0 THEN TC = TK(0): GOTO 51170'Out of bounds, round to lower
limit
51140 IF EK > NK - 2 THEN TC = TK(NK - 1): GOTO 51170 'Out of bounds,
round to upper limit
51150 'Do interpolation
51160 TC = TK(EK) + (TK(EK + 1) - TK(EK)) * (VK - EK * SIK - SVK) /
SIK'Centigrade
51170 TF = TC * 9 / 5 + 32'Fahrenheit
51180 RETURN
```

APPENDIX B. Data Evaluation Program

Program Emittance

```
C -------------------------------------------------------------------------------
C
C       This program calculates the effective emmissivity of the
C  Fabric Composite Heat Pipe.  The power (q), and temperatures
C  (Thot and Tcold) are input from the heat pipe tests. Heat loss is
C  estimated by the radiation heat transfer from the evaporator section
C  using the temperature of the heaters and the radiation shield. All
C  other data are hard wired into the code.
C
C -------------------------------------------------------------------------------
      Open (Unit=1, File = 'HP.txt')
      Print *, "Input volts, amps "
      Read *,volts,amps
      Print *, "Input Thot and Tcold (C) "
      Read *,Thot,Tcold
      Print *, "Tshield (C) "
      Read *,Tsh

C ************ Constants and heat pipe properties **********************
      qo = volts*amps
      Pi = 355./113.
      Sig = 5.6696E-8       ! Stefan-Boltzmann constant (W/m^2 K^4)
      Rss = 1.4288          ! radius of stainless heat pipe (cm)
      Rlwfc = 1.27 +.0508   ! radius of LW FC heat pipe (cm)
      Rhwfc = Rss + .0508   ! radius of HW FC heat pipe (cm)
      Rvc = 7.4613          ! radius of vacuum chamber (cm)
      zLength = 65.0        ! length of condenser section (cm)
      epsvc = 0.96          ! emissivity of the vacuum chamber
      ess = 0.3             ! emissivity for stainless steel
      rsh = 6.35            ! radius of rad shield (cm)
      eLength = 24.0        ! length of evaporator shield (cm)

C ************** Determine type of heat pipe ***************************

      Print *, "Enter 1 for SS, 2 for HWFC, 3 for LWFC "
      Read *,N
      IF (N.eq.1) THEN
```

```
 R = Rss
ENDIF
IF (N.eq.2) Then
 R = Rhwfc
ENDIF
IF (N.eq.3) Then
 R = Rlwfc
ENDIF
A = (2.*Pi*R*zLength)        ! Area of condenser section (cm^2)
Avap = (2.*Pi*Rsh*eLength)   ! Area of evaporator section (cm^2)

C *************** Unit conversions ***********************************

Th = Thot + 273.15      ! Temperature to degrees Kelvin
Tc = Tcold + 273.15
Tsh = Tsh + 273.15
A = A*1.0E-4            ! Area to m^2
Avap = Avap*1.0E-4      ! Area to m^2

C *************** Calculate blackbody power ************************

Qbb = sig*A*Th**4.

C ******************* Calculate heat loss ****************************

Tdif = Tsh**4. - Tc**4.
Ecorr = (1./ess) + ((1./epsvc)-1.)*(rsh/rvc)**2.
qloss = Sig*Avap*Tdif/Ecorr

C ***************** Correct for heat loss ****************************

q = qo - qloss

C ************** Calculation of Effective Emissivity *****************

B = Sig*A*(Th**4. - Tc**4.)
C = q*((1.-epsvc)/epsvc)*(R/Rvc)**2.
Epshp = q/(B-C)

C ************************ Print Results *****************************

Print *, "Heat input = ",qo
Print *, "Estimated heat loss = ",qloss
Print *, "Effective heat transfered = ",q
```

```
      Print *,
      Print *, "Effective Emissivity = ",Epshp


C ****************** Write results to output file ********************

       IF (N.eq.1) THEN
      Write(1,*) "Conventional Stainless Steel Heat Pipe Results "
      Endif
       IF (N.eq.2) Then
      Write(1,*) "Heavyweight Fabric Composite Heat Pipe Results "
      Endif
       IF (N.eq.3) Then
      Write(1,*) "Lightweight Fabric Composite Heat Pipe Results "
      Endif
       Write(1,*)
       Write(1,*) "-------------------------------------------------"
       Write(1,*) "Heat input = ",qo
       Write(1,*) "Estimated heat loss = ",qloss
       Write(1,*) "Effective heat transfered = ",q
       Write(1,*)
       Write(1,*) "Effective Emissivity = ",Epshp
       Write(1,*)
       Write(1,*) 'Max theoretical power = ',Qbb
       Write(1,*) 'Blackbody HP power = ',B

C ******************** Error Analysis routine ************************

       dV = 0.5
       dI = 0.05
       dTh = 2.0
       dTc = 2.0
       dTsh = 2.0
       dEss = 0.1
       depsvc = 0.04
       dqo = qo*Sqrt((dV/volts)**2. + (dI/amps)**2)

C ********* Calculate uncertainty in qloss ***************************

       dqldTsh = (4.*Sig*A*Tsh**3.)/Ecorr
       dqldTc = (-4.*Sig*A*Tc**3.)/Ecorr
       dqldess = Sig*A*Tdif/(-1./ess**2.)
       dqldevc = Sig*A*Tdif/(1./ess - (1./epsvc**2)*(R/Rvc)**2.)
```

```
      dqloss = Sqrt((dqldTsh*dTsh)**2. + (dqldTc*dTc)**2. +
     1         (dqldevc*depsvc)**2. + (dqldess*dess)**2.)


C *** Total uncertainty in Q *****
          dq = Sqrt(dqo*dqo + dqloss*dqloss)

C *********** Calculate uncertainty in emissivity **********************
      bot = B-C
      botsqr = bot*bot
      dedq = (bot-C)/botsqr
      dedTh = -4.*q*Sig*A*Th*Th*Th/botsqr
      dedTc = 4.*q*Sig*A*Tc*Tc*Tc/botsqr
      dedevc = (bot - q*(R/(Rvc*epsvc))**2.)/botsqr
      dEmiss = Sqrt((dedq*dq)**2. + (dedTh*dTh)**2. + (dedTc*dTc)**2.
     1         + (dedevc*dEpsvc)**2.)

C *************** Print Results of Error Analysis **********************

      Print *,'dqo = ',dqo
      Print *,'dqloss = ', dqloss
      Print *,'total uncertainty in q = ',dq
      Print *, 'Final uncertainty in Emissivity = ',dEmiss

C  ******************** Write results to file ***************************

      Write(1,*)
      Write(1,*) 'ERROR ANALYSIS:'
      Write(1,*)
      Write(1,*) 'Total Uncertainty in q = ',dq
      Write(1,*) 'Final uncertainty in Emissivity = ',dEmiss
      Close(1)
      End
```